Instituto Nacional de Matemática Pura e Aplicada

Backtesting SVI Parameterization of Implied Volatilities

Author: **Rafael Balestro Dias da Silva**

Advisor: **Vinícius Viana Luiz Albani**

Rio de Janeiro
July 2016

Acknowledgements

I dedicate the present work to my parents Ana and Mauro, who made it possible, to my beloved girlfriend Luiza for the understanding in relation to my constant absence, to my brother Vitor who helped me a lot with the mathematics and to my good friends Gabriela and Leonardo for the presence and great debates. Also, I would like to thank to my friends at Ancar Ivanhoe - Raphael, Luis, Pedro and Zeca - and to my friends at Vinci Partners - Renato and Tiago. A special thank to Professor Jorge Zubelli, Ph.D and to my advisor Vinicius Albani, Ph.D for all the immeasurable support during the construction of this master thesis.

Abstract

Since the stock market crash in 1987, many generalizations of Black-Scholes model have been introduced, in order to incorporate the so-called *volatility smile* effect. In this master thesis we study the numerical aspects of the stochastic volatility inspired (SVI) parameterization of implied volatility smile. Introduced at the end of 1990's, this model - which is basically a parameterized functional form - presents a nice smile adherence, which made it popular within market practitioners mainly by its low computational cost. We present numerical experiments using real data, evaluating how reliable would the fitted parameters be on calculating volatilities for future dates.

Key words: Financial Options, Financial Derivatives, Volatility Smile, Black-Scholes Formula, SVI fit, Stochastic Differential Equation, Variance Modelling.

Contents

List of Figures

List of Tables

Introduction

The price of securities such as *bonds*, *stocks* or *futures* cannot be predicted. Because it is subjected to different sources of risk and shocks, derivative contracts were introduced to protect market practitioners and companies from such randomness.

As an example, an *European call* (or *European put*) option is a contract that gives to its holder the right to buy (or sell) a given amount of an asset at a specific *maturity* time for a fixed *strike* price. In contrast, American options can be exercised at any time until its maturity. These so-called *Vanilla* options are the most liquid and intuitively reflect the market expectation of the asset price future behaviour.

More complex derivatives are key tools in hedging and trading strategies, however, they may be not sufficiently liquid to avoid arbitrage opportunities, i.e., they must be appropriately priced with mathematical models, taking into account the available market information.

In the classical Black-Scholes model [2], the dynamics of the instantaneous logarithmic of returns of an asset is given by an Itô process with constant coefficients, the asset's drift and the volatility. Under no-arbitrage arguments, European call option price is given by the well-known Black-Scholes formula.

In practice, volatility is not constant as we can see when we use Black-Scholes formula to identify it. It changes with strike and maturity. These volatilities are the so-called *implied volatilities*. The *volatility smile* can be seen when we plot such implied volatilities with the option's time to maturity fixed and vary the strike price. This name comes from its shape, since volatility usually presents lower levels for strike prices close to the underlying asset price, or *at-the-money* strikes, and higher levels as we go far from the at-the-money.

After the stock market crash in 1987, many generalizations of Black-Scholes model were proposed, where the volatility (or diffusion) coefficient is assumed stochastic. More precisely, let the asset price evolution be given by:

$$dS_t = \mu_t S_t dt + \sqrt{v_t} S_t dW_t, \ t \geq 0,$$

where μ_t is the drift, v_t the variance (the square of volatility) and $\{W_t, \ t \geq 0\}$ is a Wiener process. One possible way to model the variance v_t as a stochastic process is the following [23]:

$$dv_t = \alpha(S_t, v_t, t)dt + \tau\beta(S_t, v_t, t)\sqrt{v_t}dZ_t,$$

α and β are continuous and well-behaved functions, τ is a constant and $\{Z_t, \ t \geq 0\}$ is another Wiener process, correlated with W_t. In a first observation, this assumption clearly adds randomness sources into the model. Also, note that setting $\tau = 0$ and μ_t as a constant, we would have the standard time dependent Black-Scholes variance.

The stochastic volatility models describe in a more precise way the evolution of the underlying asset prices within a period of time. This is of particularly importance, when we want to evaluate path-dependent derivatives. However, the simulation of theses models have a higher computational cost.

A market where every contingent claim can be replicated through a portfolio of negotiable assets is called a *complete market* [16]. This is equivalent to the existence of a unique equivalent martingale measure, which gives, for example, unique European call prices. A necessary condition for this property to hold is the number of sources of uncertainty be less or equal to the number of underlying assets in a portfolio. So, a portfolio of assets modeled by stochastic volatility models fails to satisfy such condition, since the number of sources of uncertainties is in general higher than the number of assets.

Local volatility models introduced in [6] and [5], can be seen as a particular class of stochastic volatility models (see [11]), where the diffusion coefficient, or *local volatility surface*, of the asset price dynamics is a deterministic function of the underlying asset's current price and time. This model is interesting because it keeps the market completeness and the possibility of hedging positions through the derivatives. Moreover, in [6] it is proved that the local volatility is the unique diffusion coefficient consistent with quoted European option prices. However, local volatility calibration is an ill-posed inverse problem, and some regularization technique must be applied. See [4, 7, 8, 21].

Even though there is a map between local and implied volatilities, in practice, its evaluation involves a complicated tridimensional interpolation method, which is not necessarily well-behaved in terms of smoothness and continuity, since the maturity dates are discrete and sparse.

Therefore, the quest for a model which is simple and easy to calibrate, that fits the market smile and satisfies non-arbitrage conditions brought the community to study some simplifications of stochastic volatility models. Among them, there are the *stochastic volatility inspired* (SVI) models [10, 13], which consists in techniques to parametrize the implied volatility smile. It was firstly developed at Merryl Lynch in 1990 and publicly disseminated in [10].

Since it is relatively easy to implement and has interesting properties such as absence of static arbitrage, SVI models have been largely studied by the community in the past two decades. In addition, it has been shown in [12] that SVI is not arbitrary, since the large maturity limit of Heston implied volatility holds SVI non-arbitrage properties.

This master thesis aims to explore the problem of modeling implied volatility smiles in order to guarantee some important properties such as absence of calendar-spread arbitrage and static arbitrage, good fit to bid-ask implied volatilities and good behavior under extreme strikes and maturities. To do so, we will apply known SVI parameterization techniques over real data from liquidly traded European options and compare this fixed parameters with the realized implied volatilities for the next trading days.

Structure of the thesis In Chapter 1, we present the derivation of Dupire's partial differential equation and the inverse problem of local volatility surface calibration from quoted European option data through the implied diffusion process for the underlying asset's price observed from the option prices for different strikes. In Chapter 2, we make a review of theoretical results concerning SVI models. Chapter 3 is concerned with implied volatility surface modeling for real data. Some backtest techniques for market data are described in Chapter 4. In Chapter 5 we draw some concluding remarks.

Chapter 1

Local Volatility Surface and Dupire's Equation

It is well-known that the the probability density of the underlying asset price at the option's maturity time can be inferred from European vanilla option prices [3, 19]. In [6, 5], it was shown that there exists a unique state-dependent diffusion coefficient consistent with these distributions. Such parameter, denoted by $\sigma_L(S,t)$, is known as *local volatility surface*.

There are at least two interesting interpretations of local volatility surface, it can be seen as an average of all possible instantaneous volatilities in a stochastic process, this was the initial intuition of practitioners. Another one, it determines how the implied volatilities evolve, since, by no-arbitrage arguments, there is a one-to-one map between both quantities. Below, we explain both concepts.

1.1 Derivation of Dupire Equation

Suppose the stock price follows the diffusion process below:

$$\frac{dS_t}{S_t} = \mu_t dt + \sigma_L(S_t, t; S_0) dW_t,\ t \geq 0,$$

where $\{W_t,\ t \geq 0\}$ is a standard Brownian Motion, $\mu_t = r_t - D_t$ is the risk-neutral drift, given by the risk-free rate r_t minus the dividend yield D_t, and $\sigma_L(S_t, t)$ is the local volatility surface.

The undiscounted risk-neutral price $\widetilde{C} = C \exp\left(\int_t^T r_t dt\right)$ of an European option with strike K and maturity T is given by:

$$\widetilde{C}(S_0; K, T) = \mathbb{E}\left[\max\{0, S_T - K\}|S_0\right] = \int_K^\infty (S_T - K)\varphi(S_T, T; S_0) dS_T,$$

with $\varphi(S_T, T; S_0)$ the probability density of the stock price S_t at time $t = T$ (conditional to S_0). It evolves according to the Fokker-Planck equation:

$$\frac{1}{2}\frac{\partial^2}{\partial S_T^2}(\sigma_L^2 S_T^2 \varphi) - \frac{\partial}{\partial S_T}(\mu S_T \varphi) = \frac{\partial \varphi}{\partial T}.$$

Now, assuming that φ satisfies sufficient conditions such that we can differentiate under the integral sign, it follows that:

$$\frac{\partial \widetilde{C}}{\partial K} = -\int_K^\infty \varphi(S_T, T; S_0) dS_T,$$

$$\frac{\partial^2 \widetilde{C}}{\partial K^2} = \varphi(K, T; S_0),$$

and in T:

$$\frac{\partial \widetilde{C}}{\partial T} = \int_K^\infty (S_T - K) \frac{\partial}{\partial T} \varphi(S_T, T; S_0) dS_T,$$

By the Fokker-Planck equation, the later equation is equivalent to

$$\int_K^\infty (S_T - K) \left(\frac{1}{2} \frac{\partial^2}{\partial S_T^2} (\sigma_L^2 S_T^2 \varphi) - \frac{\partial}{\partial S_T} (\mu S_T \varphi) \right) dS_T.$$

Using some algebra tricks and integrating by parts twice, we find Dupire's equation:

$$\frac{\partial \widetilde{C}}{\partial T} = \frac{\sigma_L^2 K^2}{2} \frac{\partial^2 \widetilde{C}}{\partial K^2} + \mu(T) \left(\widetilde{C} - K \frac{\partial \widetilde{C}}{\partial K} \right) . \tag{1.1.1}$$

Now, we can isolate the volatility term to get the so-called Dupire's formula:

$$\sigma_L^2(K, T; S_0) = \frac{\dfrac{\partial C}{\partial T} - \mu(T) \left(\widetilde{C} - K \dfrac{\partial \widetilde{C}}{\partial K} \right)}{\dfrac{1}{2} K^2 \dfrac{\partial^2 C}{\partial K^2}}, \tag{1.1.2}$$

which is well-defined due to the static no-arbitrage condition

$$\frac{\partial^2 C}{\partial K^2} > 0$$

when $K > 0$.

This is the most important conclusions in Dupire's article [6]. In theory, the term in the right-hand of (1.1.2) can be easily evaluated with a complete set of European options prices, moreover, this represents the unique expression for local volatility surface. In what follows, we shall use equation (1.1.2) as the definition of local volatility surface. Note that, in practice, Dupire's formula is highly unstable, since we must interpolate noisy and scarce data and differentiate it, in other words, local volatility surface calibration is an ill-posed inverse problem. See [4, 7].

1.2 Local Volatility and Implied Volatility

As one could guess, it is possible to express local volatility in terms of the implied volatility, conditional to K, T and S_0, derived from the Black-Scholes formula, and denoted by $\sigma_{BS}(K, T; S_0)$. In this section, we follow [11] closely.

Firstly, define the variables:

$$F_T = S_0 \exp\left(\int_0^T \mu_t dt \right)$$

is the forward price of the stock at $t = 0$,

$$y = \log\left(\frac{K}{F_T}\right)$$

is the log-strike, and

$$\omega(S_0, y, T) = \sigma_{BS}^2(S_0, F_T e^y, T)T$$

is the Black-Scholes total implied variance. In terms of the above variables, the Black-Scholes formula for the future value of the option price becomes:

$$\begin{aligned} C_{BS}(F_T, y, \omega) &= F_T\left[\mathcal{N}(d_1) - e^y\mathcal{N}(d_2)\right] \\ &= F_T\left[\mathcal{N}\left(-\frac{y}{\sqrt{\omega}} + \frac{\sqrt{\omega}}{2}\right) - e^y\mathcal{N}\left(-\frac{y}{\sqrt{\omega}} + \frac{\sqrt{\omega}}{2}\right)\right]. \end{aligned} \tag{1.2.1}$$

Defining $u(T) = \int_t^T (r_t - D_t)\,dt$, $v(y,T) = \widetilde{C}(F_T e^y, T)$ and $\nu_L(y,T) = \sigma_L(F_T e^y, T)^2$ (the local variance), the PDE in (1.1.1) can be rewritten as:

$$\frac{\partial v}{\partial T} = \frac{\nu_L}{2}\left(\frac{\partial^2 v}{\partial y^2} - \frac{\partial v}{\partial y}\right) + \mu(T)v. \tag{1.2.2}$$

Differentiating the Black-Scholes formula in (1.2.1), we have:

$$\begin{aligned} \frac{\partial^2 C_{BS}}{\partial \omega^2} &= \left(-\frac{1}{8} - \frac{1}{2\omega} + \frac{y^2}{2\omega^2}\right)\frac{\partial C_{BS}}{\partial \omega}, \\ \frac{\partial^2 C_{BS}}{\partial y \partial \omega} &= \left(\frac{1}{2} - \frac{y}{\omega}\right)\frac{\partial C_{BS}}{\partial \omega}, \\ \frac{\partial^2 C_{BS}}{\partial y^2} &= \frac{\partial C_{BS}}{\partial y} + 2\frac{\partial C_{BS}}{\partial \omega}. \end{aligned} \tag{1.2.3}$$

Now, we want to describe equation (1.2.2) in terms of the implied variance σ_{BS}. Since, for every y and T, $v(y,T) = C_{BS}(F_T, y, \omega)$, differentiating the equation above by y and T, it follows that:

$$\frac{\partial v}{\partial y} = \frac{\partial C_{BS}}{\partial y} + \frac{\partial C_{BS}}{\partial \omega}\frac{\partial \omega}{\partial y}, \tag{1.2.4}$$

$$\frac{\partial^2 v}{\partial y^2} = \frac{\partial^2 C_{BS}}{\partial y^2} + 2\frac{\partial^2 C_{BS}}{\partial y \partial \omega}\frac{\partial \omega}{\partial y} + \frac{\partial^2 C_{BS}}{\partial \omega^2}\left(\frac{\partial \omega}{\partial y}\right)^2 + \frac{\partial C_{BS}}{\partial \omega}\frac{\partial^2 \omega}{\partial y^2}, \tag{1.2.5}$$

$$\frac{\partial v}{\partial T} = \frac{\partial C_{BS}}{\partial \omega}\frac{\partial \omega}{\partial T} + \mu(T)v. \tag{1.2.6}$$

The expression in (1.2.6) can be rewritten as:

$$\frac{\partial C_{BS}}{\partial \omega}\frac{\partial \omega}{\partial T} = \frac{\partial v}{\partial T} - \mu(T)v,$$

and by (1.2.2), the right-hand side of the above equation is equal to:

$$\frac{\partial v}{\partial T} - \mu(T)v = \frac{\nu_L}{2}\left(\frac{\partial^2 v}{\partial y^2} - \frac{\partial v}{\partial y}\right).$$

So, it follows that,

$$\frac{\partial C_{BS}}{\partial \omega}\frac{\partial \omega}{\partial T} = \frac{\nu_L}{2}\left(\frac{\partial^2 v}{\partial y^2} - \frac{\partial v}{\partial y}\right).$$

Substituting the terms $\frac{\partial^2 v}{\partial y^2}$ and $\frac{\partial v}{\partial y}$ by the expressions in (1.2.4) and (1.2.5) in the PDE (1.2.2), we have:

$$\frac{\partial C_{BS}}{\partial \omega}\frac{\partial \omega}{\partial T} = \frac{\nu_L}{2}\frac{\partial C_{BS}}{\partial \omega}\left[2 - \frac{\partial \omega}{\partial y} + \left(\frac{1}{2} - \frac{y}{\omega}\right)\frac{\partial \omega}{\partial y} + \left(-\frac{1}{8} - \frac{1}{2\omega} + \frac{y^2}{2\omega^2}\right)\left(\frac{\partial \omega}{\partial y}\right)^2 + \frac{\partial^2 \omega}{\partial y^2}\right],$$

and simplifying:

$$\frac{\partial \omega}{\partial T} = \nu_L\left[1 - \frac{y}{\omega}\frac{\partial \omega}{\partial y} + \frac{1}{4}\left(-\frac{1}{4} - \frac{1}{\omega} + \frac{y^2}{\omega^2}\right)\left(\frac{\partial \omega}{\partial y}\right)^2 + \frac{1}{2}\frac{\partial^2 \omega}{\partial y^2}\right].$$

So, we just have to invert the above equation to isolate the local variance:

$$\nu_L = \frac{\dfrac{\partial \omega}{\partial T}}{1 - \dfrac{y}{\omega}\dfrac{\partial \omega}{\partial y} + \dfrac{1}{4}\left(-\dfrac{1}{4} - \dfrac{1}{\omega} + \dfrac{y^2}{\omega^2}\right)\left(\dfrac{\partial \omega}{\partial y}\right)^2 + \dfrac{1}{2}\dfrac{\partial^2 \omega}{\partial y^2}} \tag{1.2.7}$$

The intuitive conclusion of this result is that the local variance is expressed as the forward Black-Scholes implied volatilities distorted by the skew $\frac{\partial \omega}{\partial y}$.

Even though this work doesn't aim to calibrate the local volatility surface, but the implied volatility one, this relation composes an important background to the overall understanding of the problem of pricing options using different approaches to the variance other than the constant one assumed in the Black-Scholes model.

While Dupire's result provided the discussion with a stronger theoretical background, the models which aim to interpolate and extrapolate the implied volatility surface from given market data is more straightforward and simpler to implement, with market smile adherence. Thus, the implied variance can also be expressed as a function of local volatilities.

Chapter 2

SVI Parameterization: An Introduction

Given the computational and theoretical difficulties related to the simulation of stochastic volatility models, it makes sense to search for simpler techniques that are easy to implement, arbitrage-free and that fit the market implied smile. One possible approach is the arbitrage-free interpolation for implied volatility surfaces, such as [9] and [14]. However, these models are not well suited to extrapolate the implied smile, and there is no closed-formula for volatilities. So, we choose the SVI model introduced in [10], which has a closed-form representation for the implied volatility function and guarantees the absence of static arbitrage.

In this chapter we shall present the definitions of different static arbitrage conditions and how to prevent them in the formulation of the SVI model. More precisely, we shall state sufficient conditions for the existence of a non-negative martingale defined in the probability space where European call options prices are defined as the expected value of their payoffs, under the risk-neutral measure. We shall show also that the model is free of calendar-spread arbitrage, which means that the total variance must increase with the maturity. Visually, this means that if we plot several *slices* of volatility smiles (one for each maturity time) in the same *log-strike* $\times$ *implied volatility* chart, the curves must not cross each other.

Another important characteristic that the SVI model has is the consistency with respect to Roger Lee's moment formula [18], which set bounds for the tail slopes of implied volatility at extreme maturities.

2.1 Roger Lee's Moment Formula

In [18], the author presented the *moment formula of implied volatilities*, which implies some properties of the implied volatility tail slopes at large and small-strikes, setting bounds for these slopes, which can be interpreted as arbitrage bounds. We shall review these results.

Let us recall the notation

$$y = \log\left(\frac{K}{F_T}\right), \quad \text{and} \quad \omega(y) = \sigma^2_{BS}(S_0; y, T)T,$$

where the latter is the total implied variance of Black-Scholes model for a given maturity T. Let β be defined by $\beta|y|/T = \omega(y)$.

Roger Lee's moment formula shows that, when calculating

$$\beta_R = \limsup_{y\to\infty} \beta \quad \text{and} \quad \beta_L = \limsup_{y\to-\infty} \beta,$$

it follows that $\beta_R, \beta_L \in [0, 2]$. Also, it states the following:

Theorem 1 (Roger Lee's Moment Formula for Implied Volatility)**.**

$$\frac{1}{2\beta_R} + \frac{\beta_R}{8} - \frac{1}{2} = \sup\left\{p : \mathbb{E}[S_T^{1+p}] < \infty\right\},$$

and

$$\frac{1}{2\beta_L} + \frac{\beta_L}{8} - \frac{1}{2} = \sup\left\{q : \mathbb{E}[S_T^{-q}] < \infty\right\}.$$

In [18], the theorem above is proved when the asset S_T has an arbitrary distribution.

Theorem 1 shows that the best constant for the tails slopes depend only on the number of finite moments of the distribution of the underlying asset.

Despite we shall not give the complete proof of Theorem 1 since it is not the focus of the present work, we shall demonstrate two important lemmas that help us to understand why SVI parameterization is consistent with Roger Lee's moment formula.

Define $\beta_0 = \exp\left(-\int_0^T \mu_t dt\right)$ as a discount factor and write the Black-Scholes option price for the strike $K(y)$ as $\hat{C}(K(y)) = C_{BS}(y, \omega(y))$, where $K(y) = F_T \exp(y)$ is the strike at the log-moneyness y. We have the following lemmas:

Lemma 1. *There exists $y^* > 0$ such that for every $y > y^*$,*

$$\omega(y) > \sqrt{2|y|/T}.$$

Proof. Since C_{BS} is strict monotone, the lemma follows from this:

$$C_{BS}(y, \omega(y)) < C_{BS}(y, \sqrt{2|y|/T}),$$

If $x > x^*$. On the left hand side of the above equation we have:

$$\lim_{y\to\infty} \hat{C}(K(y)) = \lim_{K\to\infty} \beta_0 \mathbb{E}(S_T - K)^+ = 0,$$

which is guaranteed by the Dominated Convergence Theorem, since $\mathbb{E}(S_T - K)^+ < \infty$. By L'Hôpital rule, the right-hand limit can be written as:

$$\lim_{y\to\infty} C_{BS}(y, \sqrt{2|y|T}) = \beta_0 F_T \left[\Phi(0) - \lim_{y\to\infty} \exp(y)\Phi(-\sqrt{2y|})\right] = \beta_0 F_T/2,$$

which completes the proof. □

Lemma 2. *For any $\beta > 2$ there exists y^* such that for all $y < y^*$,*

$$\omega(y) > \sqrt{\beta|y|/T}.$$

Hence, for $\beta = 2$ the conclusion holds if and only if $\mathbb{P}(S_T = 0) < 1/2$.

Proof. For $\beta > 2$ there exists y^* such that for all $y < y^*$,

$$\mathbb{P}(S_T < F_T \exp(y)) < \Phi(-\sqrt{f_-(\beta)|y|}) - \exp(-y)\Phi(-\sqrt{f_+(\beta)|y|}),$$

where f is the characteristic function of the underlying asset's price at $t = T$.

The stated above is true since, as $y \to \infty$ the second part converges to $\mathbb{P}(S_T = 0)$, and the first part approaches 1 (or 1/2 in case $\beta = 2$ for the special case stated in the lemma). Therefore, due to the strict monotonicity of the Black-Scholes price of an European put option P_{BS}:

$$P_{BS}(y, \omega(y)) = \beta_0 \mathbb{E}(K(y) - S_T)^+ \leq \beta_0 K(y) \mathbb{P}(S_T < F_T \exp(y)) < P_{BS}(y, \sqrt{\beta |y|/T}),$$

for all $y < y^*$. □

The stated above shows that the large and small tails slopes are not larger than 2 and, as a consequence, the implied Black-Scholes variance is linear in the log-strike y as $|y| \to \infty$. These are characteristics that the SVI parameterization must hold.

2.2 Static Arbitrage

We want to find an implied volatility surface that is free of static arbitrage, which means that there exists a non-negative martingale model such that:

$$\widetilde{C}(K, T) = \mathbb{E}^{\mathbb{Q}}[(S_T - K)^+],$$

that is, the undiscounted European call option price at maturity can be written as the expected value of its final payoff in the risk-neutral measure $\mathbb{Q}$ for some process S_t.

Definition 1. *A volatility surface ω is free of static arbitrage if and only if:*

(i) *is free from calendar spread arbitrage;*

(ii) *is free of butterfly arbitrage at each single time slice.*

Note that, Item *(i)* of Definition 1 guarantees the monotonicity of European call option prices with respect to theirs maturities, while Item *(ii)* guarantees the existence of a probability density. For more information about static arbitrage and implied volatilities, please see [20]. From now on this chapter shall review some theoretical aspects exposed in [13].

2.2.1 Calendar Spread Arbitrage

Consider two European call options of strike K and maturities T_1 and T_2 with $T_1 > T_2$. Since $T_1 > T_2$ we would intuitively expect that the price of the option with the larger maturity is higher than the other one. That happens because the more time we have ahead, the more uncertainty we suppose we will be exposed, so we would expect a higher total variance, therefore a higher price. That is why, whenever this condition is not respected, the calendar spread arbitrage is characterized.

In order to have an accurate model to price options, one would suppose that this condition must be respected, that is, the implemented model must guarantee monotonicity for the call options with same strike and different maturities. That leads us to the following definition:

Definition 2. *A volatility surface ω is free of calendar spread arbitrage if*

$$\frac{\partial \omega}{\partial t}(y, t) \geq 0,$$

for all $y \in \mathbb{R}$ and $t > 0$.

This definition is motivated by the following lemma:

Lemma 3. *Considering a constant proportional to the underlying asset prices dividends (if applicable), the volatility map ω is free of calendar spread arbitrage if and only if:*

$$\frac{\partial \omega}{\partial t}(y,t) \geq 0,$$

for all $y \in \mathbb{R}$ and $t > 0$.

Proof. Let $(X_t)_{t\geq 0}$ be a martingale and $L \geq 0$, $0 \leq t_1 < t_2$. Then, the following relation is true:

$$\mathbb{E}[(X_{t2} - L)^+] \geq \mathbb{E}[(X_{t1} - L)^+]$$

Now, let $\widetilde{C}_1$ and $\widetilde{C}_2$ be options with strikes K_1 and K_2, and maturities t_1 and t_2, respectively, and with the same log-strike or log-moneyness:

$$\frac{K_1}{F_{t_1}} = \frac{K_2}{F_{t_2}} = \exp(y)$$

Then, the process $\{X_t\}_{t\geq 0}$ defined by $\frac{S_t}{F_t}$ for $t \geq 0$ is a martingale and we have the following relation:

$$\frac{\widetilde{C}_2}{K_2} = \exp(-y)\mathbb{E}[(X_{t_2} - \exp(y))^+] \geq \exp(-y)\mathbb{E}[(X_{t_1} - \exp(y))^+] = \frac{\widetilde{C}_1}{K_1},$$

if the dividends are proportional. □

This relation means that, for constant *moneyness*, option prices are non-decreasing in time to maturity. If this relation stands for Black-Scholes prices $C_{BS}(y, \omega(y,t))$ then, $\omega(y,t)$ is strictly increasing.

2.2.2 Butterfly Arbitrage

In this subsection we shall define butterfly arbitrage over a time slice of the volatility surface. Thus, we shall use $\omega(y)$ in order to simplify the notation, since the time will be hold fixed. Now, recalling the Black-Scholes formula:

$$C_{BS}(y, \omega(y)) = S(\mathcal{N}(d_+(y)) - \exp(y)\mathcal{N}(d_-(y))), \text{ for all } y \in \mathbb{R}$$

with $\mathcal{N}$ the Gaussian cumulative distribution function and $d_\pm(y) := -y/\sqrt{\omega(y)} \pm \sqrt{\omega(y)}/2$.

Now, let $g : \mathbb{R} \to \mathbb{R}$ be a function defined by:

$$g(y) := \left(1 - \frac{y\omega'(y)}{2\omega(y)}\right)^2 - \frac{\omega'(y)^2}{4}\left(\frac{1}{\omega(y)} + \frac{1}{4}\right) + \frac{\omega''(y)}{2}. \tag{2.2.1}$$

Definition 3. *A volatility map $y \to \omega(y)$ given for some maturity is free of butterfly arbitrage if the corresponding asset's probability density is non-negative. Please refer to the 1 for the realtion between $\omega(y)$ and the underlying asset probability density.*

Lemma 4. *A volatility map $y \to \omega(y)$ given for some maturity is free of butterfly arbitrage if and only if $g(y) \geq 0$ for all $y \in \mathbb{R}$ and $\lim_{y\to\infty} d_+(y) = -\infty$.*

Proof. As mentioned in Chapter 1, the probability density function φ can be inferred from a set of option prices by:

$$\varphi(y) = \frac{\partial^2 C(y)}{\partial K^2} = \frac{\partial^2 C_{BS}(y, \omega(y))}{\partial K^2},$$

for any $y \in \mathbb{R}$ and $K = F_t \exp(y)$.

Now, differentiating the Black-Scholes formula, for any $y \in \mathbb{R}$ we have:

$$\varphi(y) = \frac{g(y)}{\sqrt{2\pi\omega(y)}} \exp\left(-\frac{d_-(y)^2}{2}\right).$$

It is important to notice that this density function may not always have its integral equals 1. In particular, call prices must go to 0 as $y \to \infty$, which is equivalent to the second part of Lemma 4. □

2.3 Different SVI Formulations for Implied Volatility Slices

In this section we shall present different functional forms which have been proposed to fit the implied volatility curve for a given maturity with real data.

Firstly, we shall see the raw SVI parameterization, which was introduced in [10], then we will present an alternative (and equivalent) parameterization so-called natural SVI parameterization. We shall not discuss the SVI-JW (Jump-Wing) parameterization since we are interested in time independent methods for backtesting in different dates.

2.3.1 The Raw SVI Parameterization

Let $\chi_R = \{a, b, \rho, m, \sigma\}$ be a set of parameters. The raw SVI parameterization of total implied variance is:

$$\omega(y; \chi_R) := a + b\left[\rho(y - m) + \sqrt{(y - m)^2 + \sigma^2}\right], \tag{2.3.1}$$

where $b \geq 0$, $|\rho| < 1$, $a \in \mathbb{R}$, $\sigma > 0$, and $a + b\sigma\sqrt{1 - \rho^2} \geq 0$ to guarantee that $\omega(y; \chi_R) \geq 0$ for all $y \in \mathbb{R}$. It is easy to see that for a given set χ_R, the function $y \to \omega(y, \chi_R)$ is strictly convex.

Now, we will investigate the intuitive meaning of the formulation parameters χ_R through the derivatives of equation ω in (2.3.1):

$$\begin{aligned}
\frac{\partial \omega}{\partial a} &= 1, \\
\frac{\partial \omega}{\partial b} &= \rho(y - m) + \sqrt{(y - m)^2 + \sigma^2}, \\
\frac{\partial \omega}{\partial \rho} &= b(y - m), \\
\frac{\partial \omega}{\partial m} &= \frac{m - y}{\sqrt{(y - m)^2 + \sigma^2}} - b\rho, \\
\frac{\partial \omega}{\partial \sigma} &= \frac{\sigma}{\sqrt{(y - m)^2 + \sigma^2}}.
\end{aligned}$$

Figure 2.1 shows a generic raw SVI curve with the set of parameters $\chi_R = (0.05, 0.15, 0.40, 0.30, 0.45)$. Figures 2.2-2.6 illustrate how variations on each parameter may change the shape of the volatility curve.

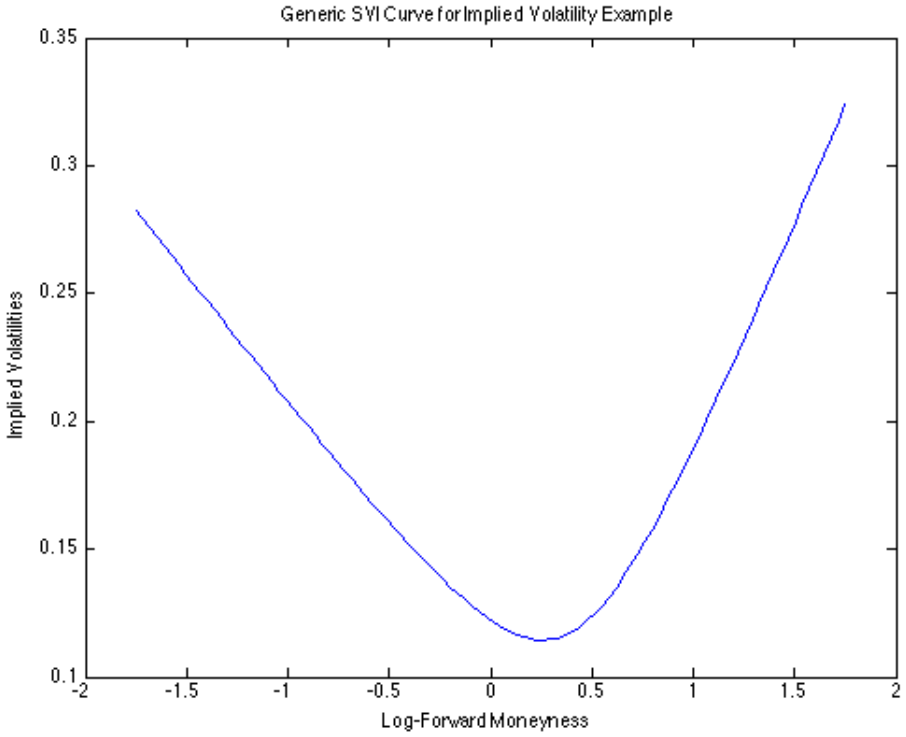

Figure 2.1: Generic Curve Shape of a Raw SVI Parameterization

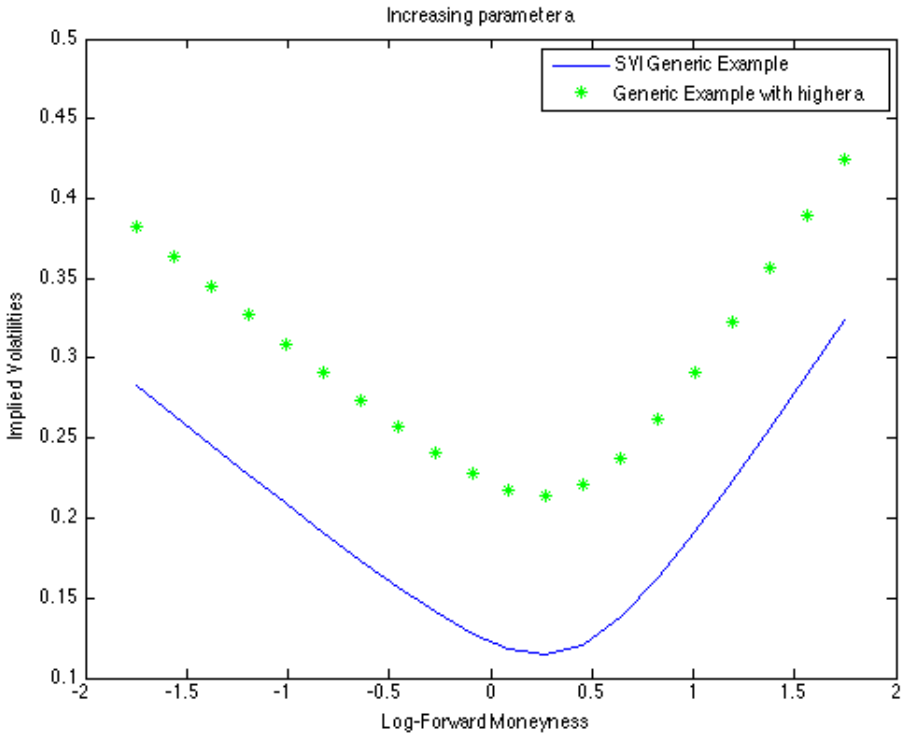

Figure 2.2: Increasing parameter a

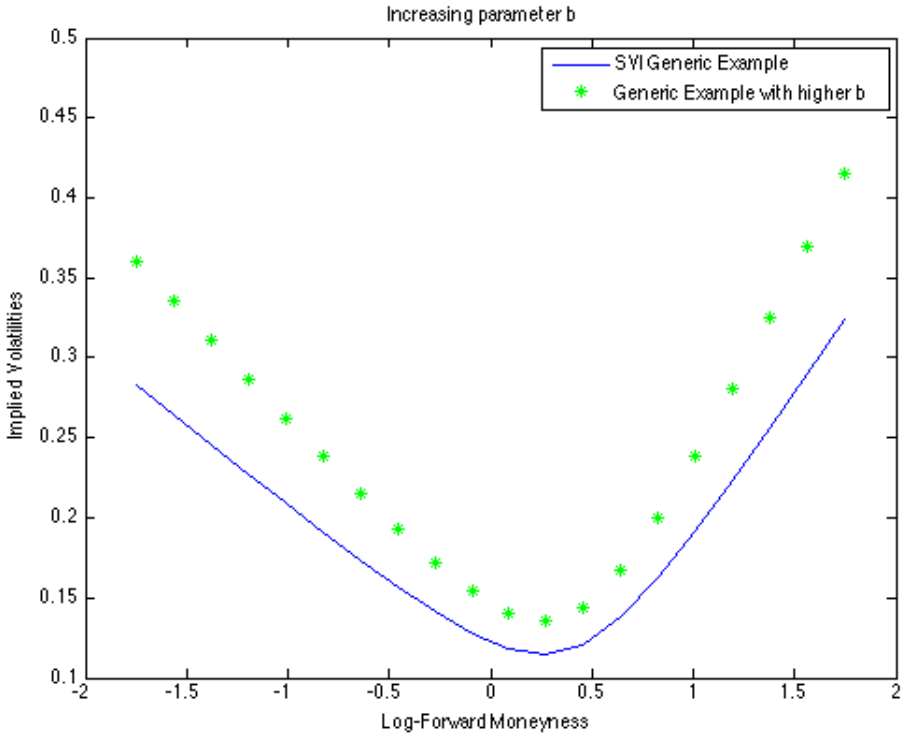

Figure 2.3: Increasing parameter b

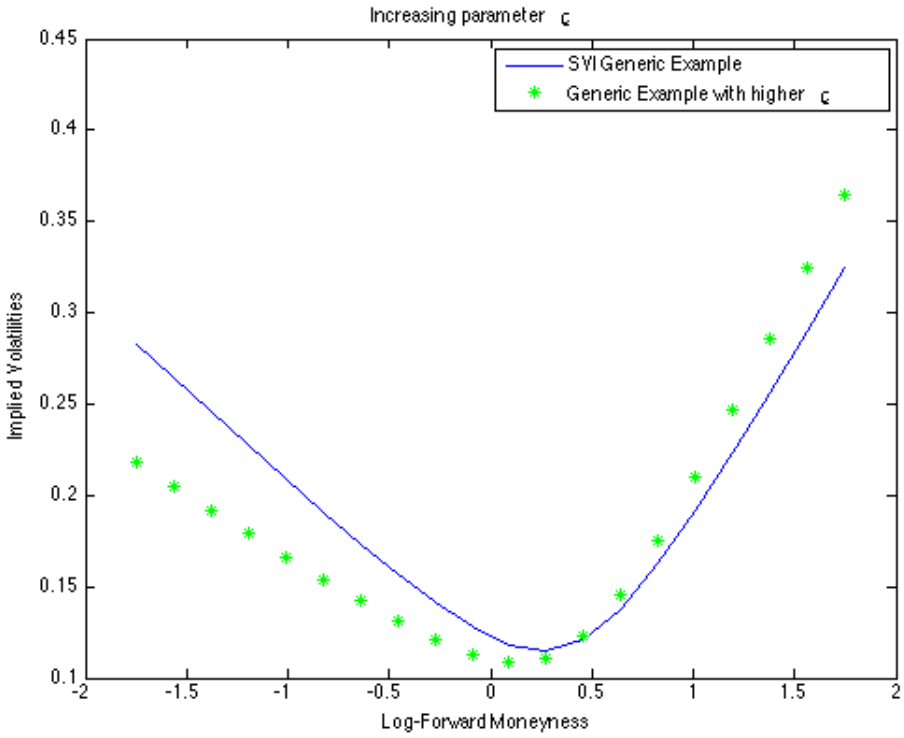

Figure 2.4: Increasing parameter ρ

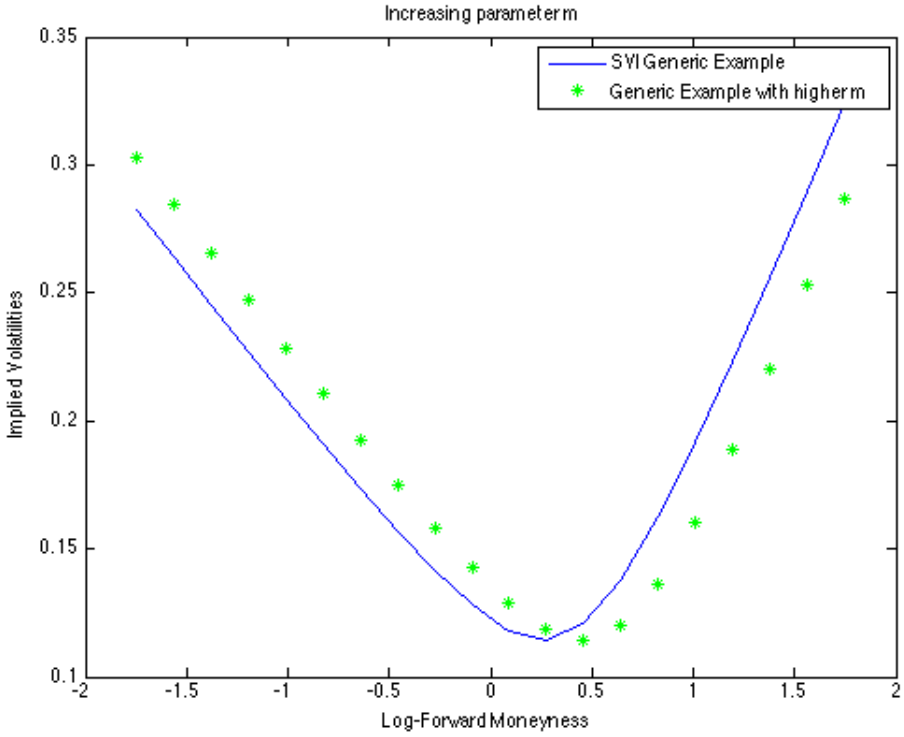

Figure 2.5: Increasing parameter m

As you can see in Figures 2.2, 2.3, 2.4, 2.5 and 2.6,

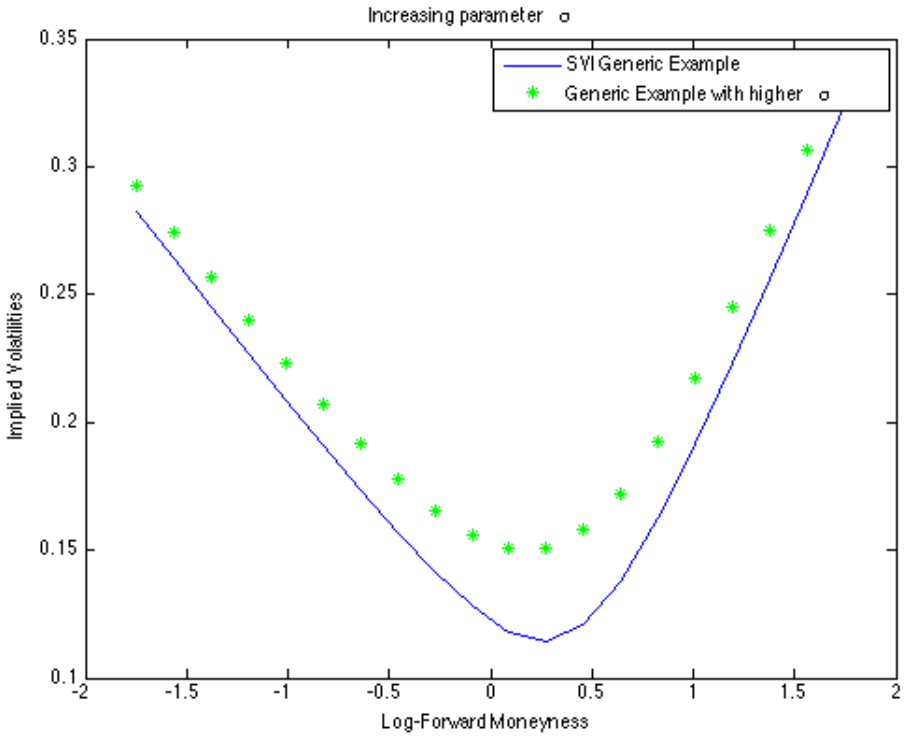

Figure 2.6: Increasing parameter σ

- when a increases, the level of total variance also increases, that is, there is a vertical translation of the curve;
- increasing b, the slopes of the put and call wings also increase, which represents an increase of total variance for *out-of-money* strikes;
- when ρ increases, there is a reduction of the call wing total variance;
- changing m, there is a translation of the curve in the x axis;
- increasing ω, the curvature reduces in the neighborhood of the *at-the-money* strike.

2.3.2 The natural SVI parameterization

The natural SVI parameterization

$$\omega(y;\chi_R) = \Delta + \frac{w}{2}\left\{1 + \zeta\rho(y-\mu) + \sqrt{(\zeta(y-\mu)+\rho)^2 + (1-\rho^2)}\right\}, \tag{2.3.2}$$

is equivalent to the raw SVI by the following change of variables:

$$(a,b,\rho,m,\sigma) = \left(\Delta + \frac{w}{2}(1-\rho^2), \frac{\zeta w}{2}, \rho, \mu - \frac{\rho}{\zeta}, \frac{\sqrt{1-\rho^2}}{\zeta}\right). \tag{2.3.3}$$

Note that, now there are two "level variables", Δ which has a straight unitary derivate, and w which doesn't have, while in the raw formulation the only "level variable" a has unitary derivate.

Chapter 3

Parameters Modelling and Preliminary Results

The goal of this chapter is to find a stable and reliable way to calibrate the raw SVI parameters in (2.3.1) for a given set of implied volatilities observed in the market. It is well known that the least square technique for this problem is affected by the large quantity of local minima. Other problem regarding this modeling is that optimizing over a 5-dimensional set of parameters usually returns non-stable results.

Therefore, the technique which will be applied is the one presented in [22] with a small modification developed for us in order to make the choice of m and σ more precise. This approach is particularly interesting because it simplifies the problem dividing it into one linear programming and one two-dimension equation optimization through a simple dimensional reduction. Moreover, the results are impressively good and the computational cost is low, if compared to other techniques such as stochastic volatility models.

3.1 The Algorithm

Let $\omega_{Total} = \omega T$ be the total variance. Now, applying the following change of variable on the log-strikes:

$$x = \frac{y - m}{\sigma},$$

we turn the SVI parameterization into:

$$\omega_{Total}(x) = aT + b\sigma T(\rho x + \sqrt{x^2 + 1}).$$

The equation above shows that, for fixed values of m and σ, the SVI curve is completely specified by a, σb and ρ. Hence, if we define the parameters:

$$c = b\sigma T,$$
$$d = \rho b\sigma T,$$
$$A = aT,$$

then we rewrite SVI formulation such that it is linear in the variables A, c and d:

$$\omega_{Total}(x) = A + dx + c\sqrt{x^2 + 1}$$

It is important to note that the region where the parameters A, c and d are defined must respect the original parameters boundaries, so it is derived from these constraints. Define the parallelepiped D:

$$D = \left\{(A, c, d) \in \mathbb{R}^3 \ : \ A \in \mathbb{R}, \ c \geq 0, \ d \in \mathbb{R}\right\},$$

which is the region in $\mathbb{R}^3$ where these new variables are defined. Therefore, for a given set of n market observation pairs $(x_i, \omega^{mkt}_{Total(i)})$, we define the cost function as:

$$f_{(x_i, \omega^{mkt}_{Total(i)})}(A, c, d) = \sum_{i=1}^{n} \left(A + dx_i + c\sqrt{x_i^2 + 1} - \omega^{mkt}_{Total(i)} \right)^2.$$

So, it is only necessary to find the triplet (A^*, c^*, d^*) for which $\nabla f = 0$ and then solve the problem P below with the corresponding triplet (a^*, b^*, ρ^*):

$$(P) \qquad \min_{m,\sigma} \sum_{i=1}^{n} (\omega_{m,\sigma,a^*,b^*,\rho^*}(y_i) - \omega_{market(i)})^2.$$

The objective function in the optimization problem above is so-called *sum of the squared errors*. Its square root is so-called *RMSE*.

3.2 The Implementation

The algorithm presented above is strongly dependent on the initial guesses of m and σ, i.e., it is a heuristic method. Therefore, in order to reduce such dependence, the algorithm must be tested with different initial values of m and σ, in order to choose appropriately the initial guesses. More precisely, the minimization is initialized with all combinations of m and σ ranging from 0.01 to 0.99, with the step size 0.01. We choose the pair that presents the lower *RMSE* values. This adds some computational cost to the problem but not sufficient to become a problem, since each calibration takes around 2-3 minutes to be performed.

Also, a loop structure with 10 iterations has been applied for every pair of initials (m, σ). The MATLAB© code of the function created to calibrate these parameters can be found in Appendix 5.

Note that, the *bid-ask spread* is not always well-behaved, mainly when we go far from the *at-the-money* strikes. To overcome this issue, we exclude the *outliers*, since they do not add relevant information to the analysis and usually are related to low trading volume options.

3.3 Illustrative Results

Before implementing a backtest strategy for the fitted parameters, we illustrate the smile adherence of the SVI parameterization. The data is composed by SPX index options traded at 13th, 14th and 15th of October, 2015, with the shortest maturity time available - 21th of October. The resulting SVI curves compared with the market implied volatilities can be found in Figures 3.1, 3.2 and 3.3.

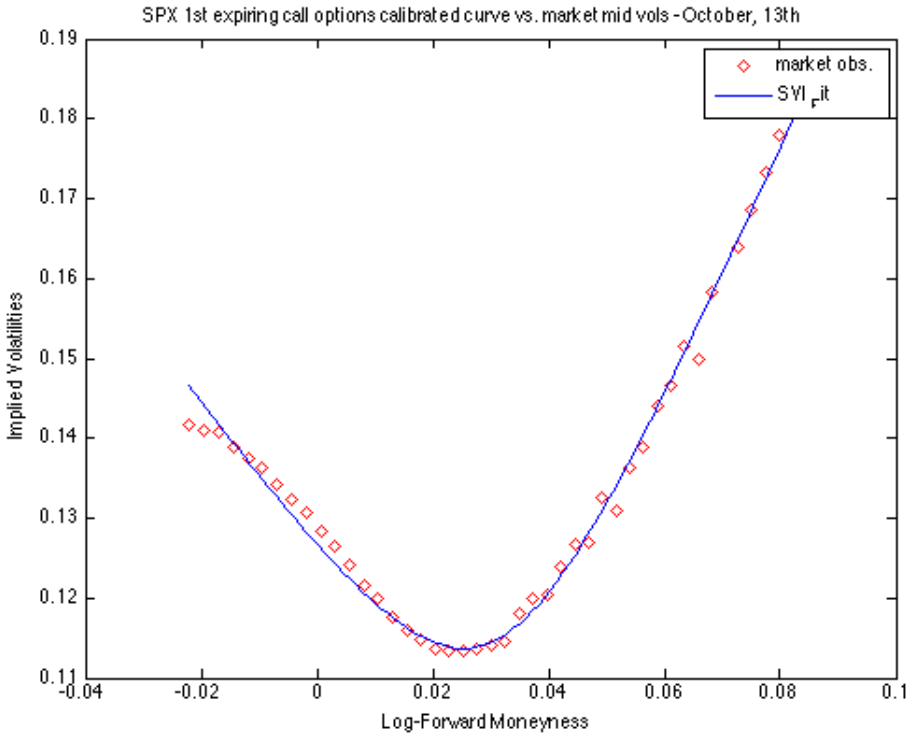

Figure 3.1: SPX Implied Volatility Curve at October, 13th 2015

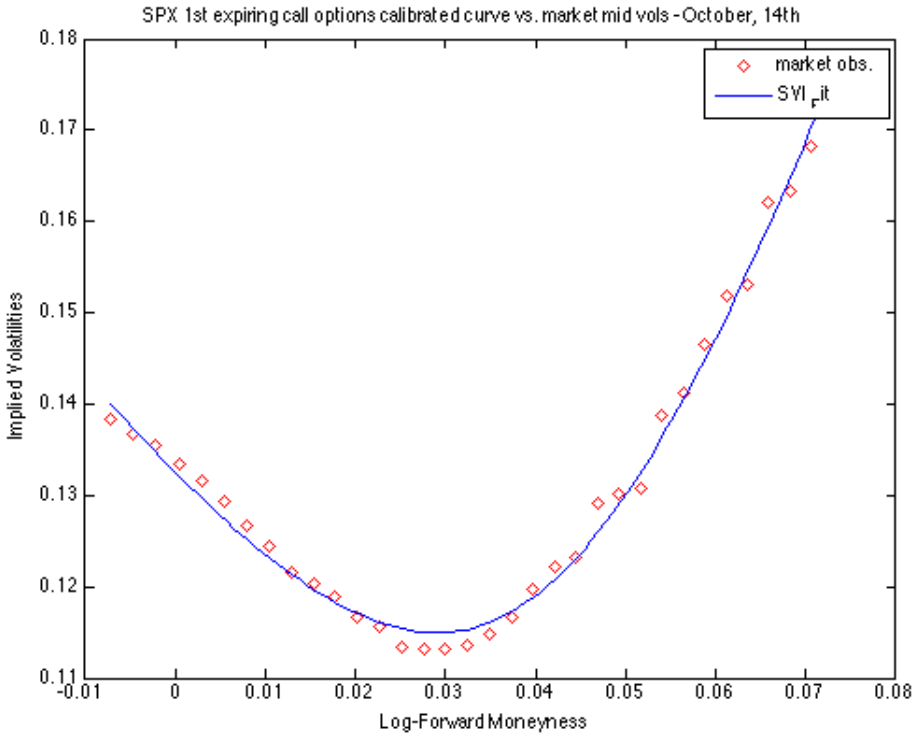

Figure 3.2: SPX Implied Volatility Curve at October, 14th 2015

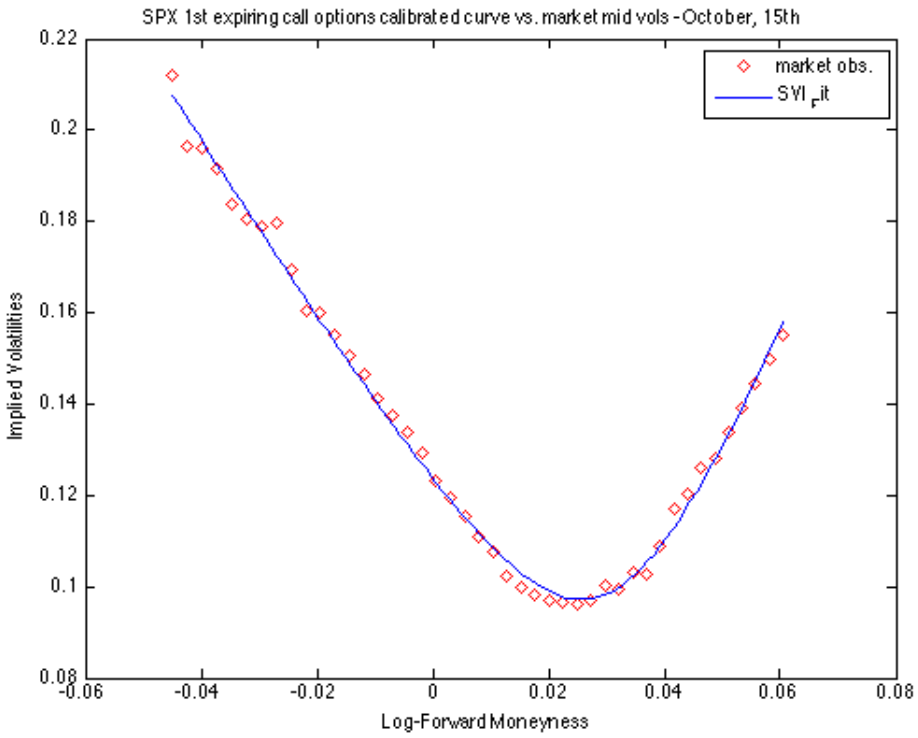

Figure 3.3: SPX Implied Volatility Curve at October, 15th 2015

	a	b	m	ρ	σ	RMSE
SPX calls at October, 13th	0.0872	1.3634	0.0302	0.2365	0.0200	$1.18x10^{-2}$
SPX calls at October, 14th	0.0537	2.1805	0.0399	0.3435	0.0299	$0.90x10^{-3}$
SPX calls at October, 15th	0.0463	2.6030	0.0299	0.2067	0.0200	$1.60x10^{-2}$

Table 3.1: Calibrated Parameters for the Example Curves

Table 3.1 presents the parameters values calibrated from the SPX data and used to find the SVI curves plotted in Figures 3.1-3.3. As one can see, the curves fit the market data well and the *RMSE* is low.

Chapter 4

Backtesting SVI

After presenting the SVI parameterization, now, we shall backtest it. More precisely, we shall verify how accurate it is as a prediction method.

4.1 Backtesting Methodology

We use the following market data:

- Underlying asset *end of the day* price;
- Risk-free interest rate (annualized);
- Evaluate the forward price corresponding to the underlying asset (based on the *end of the day* price and the risk-free interest rate);
- Time to maturity (in years);
- European call and put bid and ask prices for every strike with negotiations on the date.

Using the data above, it is possible to calculate the Black-Scholes implied volatility corresponding to the bid and ask prices, and calibrate the raw SVI (2.3.1) parameters through the algorithm described in 3. Once the parameters are identified, we apply two different tests that verify non-arbitrage properties. The first one is to test butterfly arbitrage, where the function defined in (2.2.1) must be non-negative in $\mathbb{R}$. The second one is to test Roger Lee's extreme slope (1) conditions, where we take into consideration the largest and smallest log-strikes in the data.

Now, we can calculate implied volatilities for any log-strike using the SVI function. So, we can price any option on the considered asset/maturity pair at any time we want. In what follows, we test how accurate the calibrated SVI curve is to predict option prices at future dates. If D denotes the negotiation date considered in calibration, we evaluate option prices at the dates D+1, D+3 and D+5, comparing them with market prices. We plot the corresponding implied volatilities of the model prices with market bid and ask prices. The prediction is considered accurate if the model implied volatilities fall between the market bid and ask ones. These results shall be presented in the subsequent subsections.

The following functions are used to measure the distance between model prices and data, i.e., how accurate the model is:

- Data misfit for volatilities:

$$\sqrt{\frac{\sum_{i=1}^{n}\left(\sigma_i^{SVI}-\sigma_i^{Market}\right)^2}{\sum_{i=1}^{n}\left(\sigma_i^{Market}\right)^2}},$$

where n is the total number of log-strikes in the data, σ^{SVI} is the SVI implied volatility and σ^{Market} is the implied volatility of the mean of market bid and ask prices.

- Normalized ℓ_2-error of prices:

$$\sqrt{\frac{\sum_{i=1}^{n}\left(C_i^{SVI}-C_i^{Market}\right)^2}{\sum_{i=1}^{n}\left(C_i^{Market}\right)^2}},$$

where C^{SVI} is the Black-Scholes option price calculated with the SVI volatility for each log-strike.

- Average error over spot:

$$\frac{\left[\sum_{i=1}^{n}\left(C_i^{SVI}-C_i^{Market}\right)\right]}{nS_0},$$

where S_0 is the underlying asset spot price.

4.2 DAX Index spot options

DAX Index European type options are traded daily at *Eurex Exchange* in EUR currency and have a high volume of trading, so it matches our requirements for the test. We took all the necessary data for call and put options on D =22-Jan-2016, and then, we fitted the curve and tested the non-arbitrage properties. The fitted parameters can be found in Table 4.1.

Figures 4.1 and 4.3 show the calibrated SVI curve for DAX Index options expiring in 15-Mar-2016. Note that, the fitted curve for put options in Figures 4.3 is not free of butterfly arbitrage, since the function $g(y)$ defined in (2.2.1), and plotted in Figure 4.4 has negative values. It can also be observed in Figure 4.3, since one can notice that the curve presents non-desirable concavity. The same does not happen with call prices, as we can see in Figures 4.1 and 4.2, where the volatility curve is convex and the function $g(y)$ is non-negative.

	a	b	m	ρ	σ
DAX Index Spot Call Options	0.1083	48.6448	0.1600	0.9807	0.0100
DAX Index Spot Put Options	0.2552	-0.2282	0.01	4.0272	0.0303

Table 4.1: Calibrated Parameters for DAX Index Spot Options

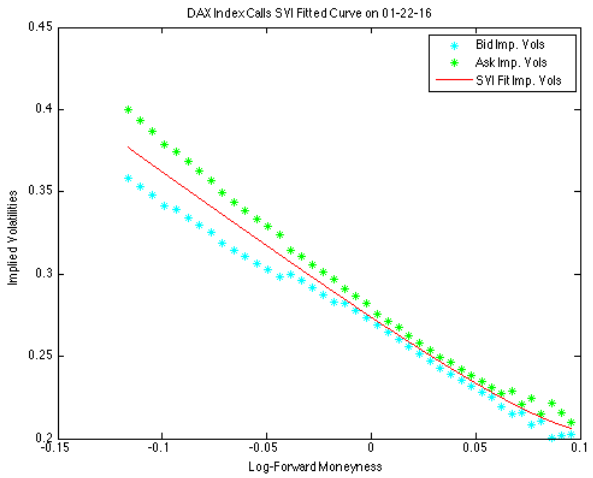

Figure 4.1: DAX Index Call Options' SVI Fitted Curve (expiring: March/16)

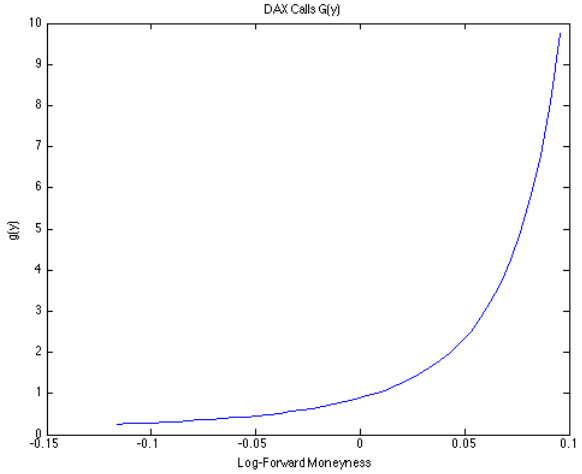

Figure 4.2: g(y) function for DAX Index Calls Options SVI Fit

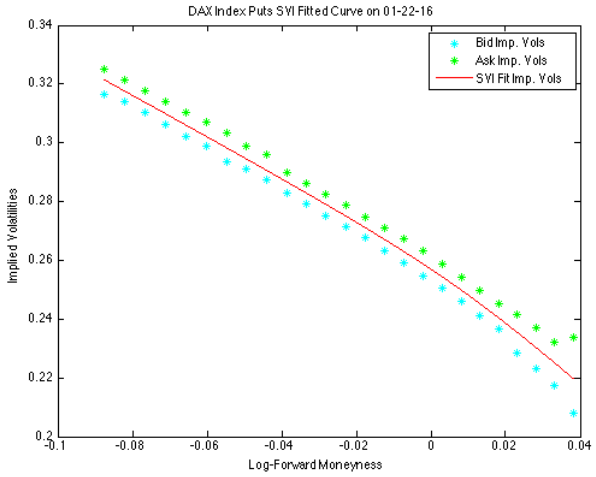

Figure 4.3: DAX Index Put Options' SVI Fitted Curve (expiring: March/16)

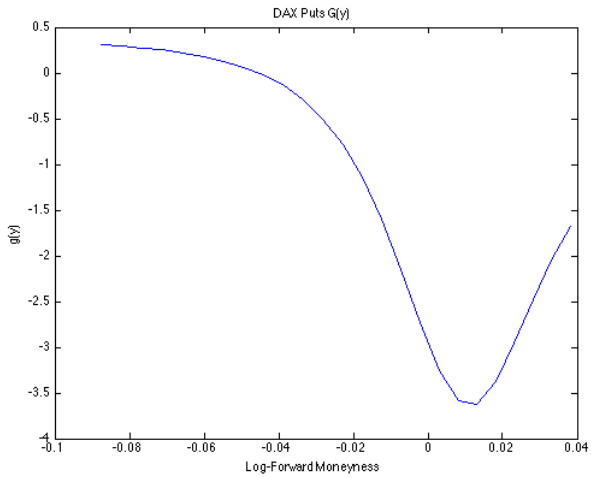

Figure 4.4: g(y) function for DAX Index Puts Options SVI Fit

4.2.1 Backtest Results for DAX Index Spot Options

Figures 4.6, 4.10, 4.14, 4.8, 4.12 and 4.16 show the comparison between market prices and the predicted prices at the dates $D+1$, $D+3$ and $D+5$. The predictions are evaluated with the SVI volatilities calibrated at D.

Figures 4.5, 4.9, 4.13, 4.7, 4.11 and 4.15 compares market implied volatilities of bid and ask prices and the volatilities of prices predicted by the SVI model.

Even though the SVI volatilities curve do not fall perfectly inside the *bid-ask* spread, the predicted prices presented good adherence to the market ones.

Calls	D+1	D+3	D+5
Data misfit for vols.	$1.07.10^{-1}$	$1.53.10^{-1}$	$2.3.10^{-1}$
Normalized ℓ_2-error of prices	$2.31.10^{-1}$	$6.02.10^{-2}$	$9.76.10^{-2}$
Average error over spot	$1.01.10^{-3}$	$3.20.10^{-3}$	$4.10.10^{-3}$
Puts	D+1	D+3	D+5
Data misfit for vols.	$3.25.10^{-2}$	$3.02.10^{-2}$	$4.76.10^{-2}$
Normalized ℓ_2-error of prices	$3.40.10^{-2}$	$3.84.10^{-2}$	$4.87.10^{-2}$
Average error over spot	$8.20.10^{-4}$	$5.45.10^{-4}$	$6.93.10^{-4}$

Table 4.2: Quantitative Indexes for DAX Index Spot Options

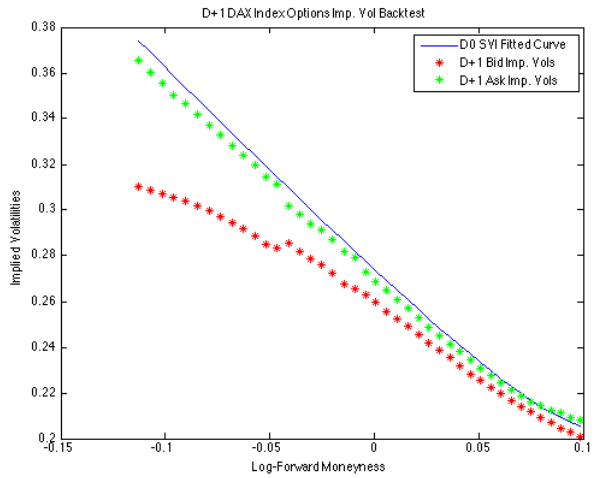

Figure 4.5: D+1 Market vs SVI Implied Vols. Comparison for DAX Call Options

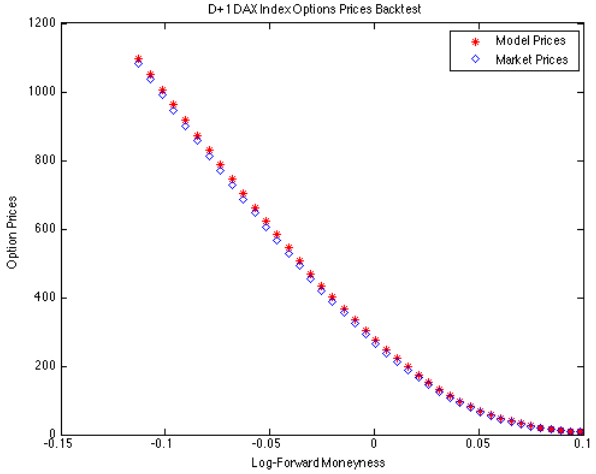

Figure 4.6: D+1 Market Prices vs Model Prices Comparison for DAX Call Options

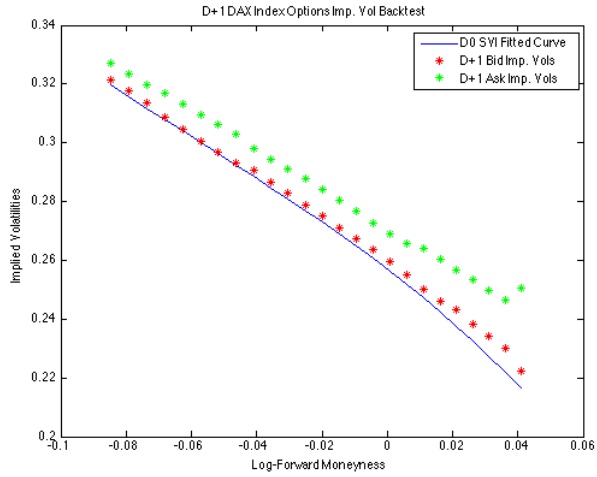

Figure 4.7: D+1 Market vs SVI Implied Vols. Comparison for DAX Put Options

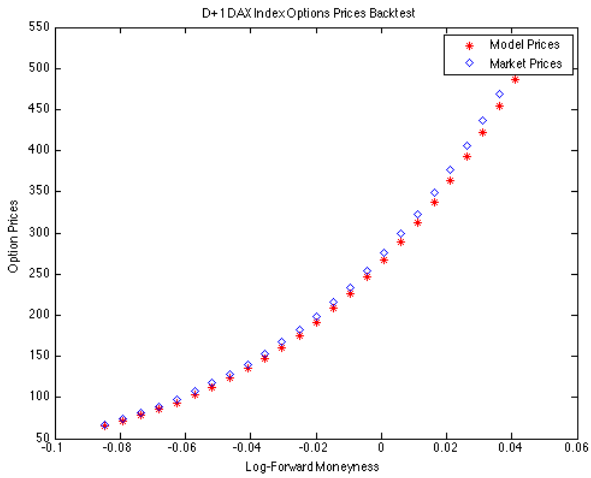

Figure 4.8: D+1 Market Prices vs Model Prices Comparison for DAX Put Options

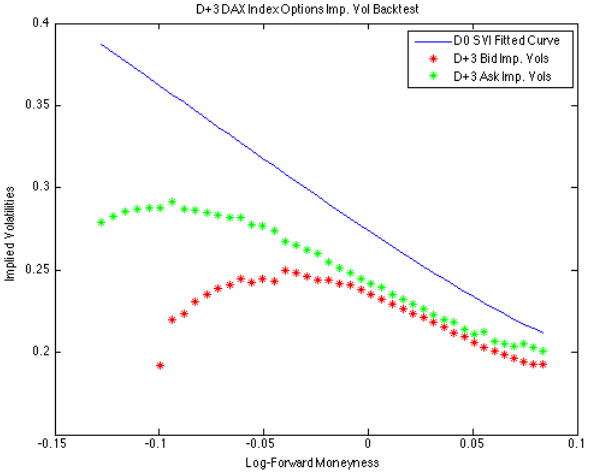

Figure 4.9: D+3 Market vs SVI Implied Vols. Comparison for DAX Call Options

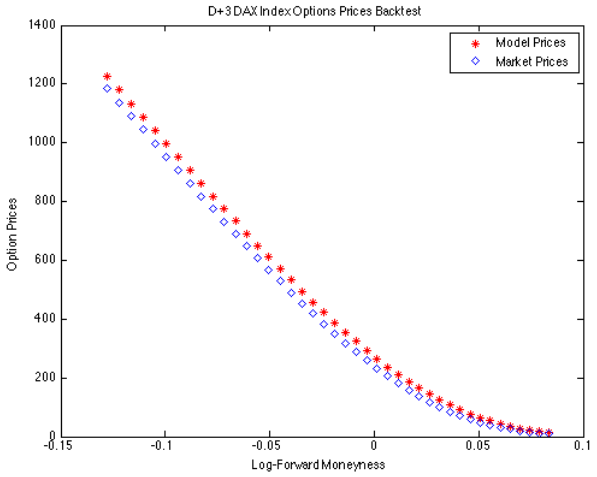

Figure 4.10: D+3 Market Prices vs Model Prices Comparison for DAX Call Options

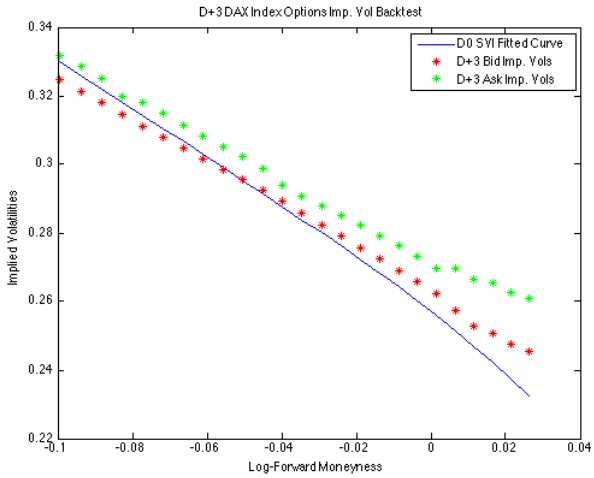

Figure 4.11: D+3 Market vs SVI Implied Vols. Comparison for DAX Put Options

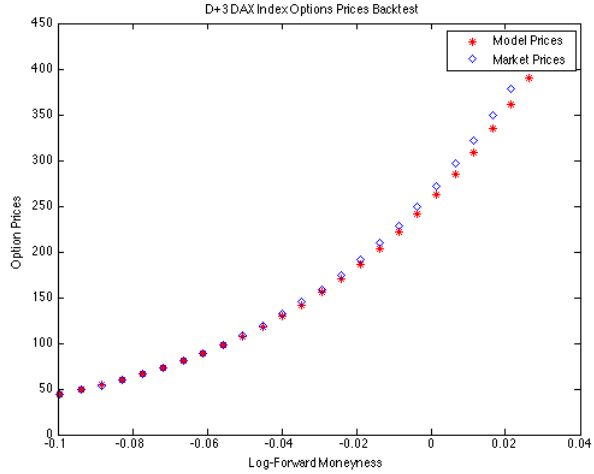

Figure 4.12: D+3 Market Prices vs Model Prices Comparison for DAX Put Options

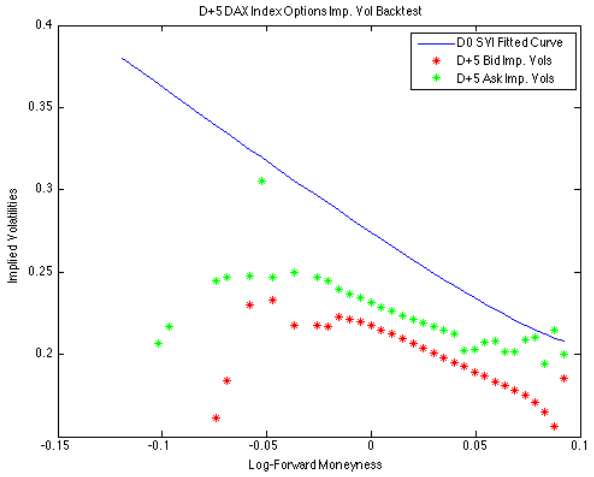

Figure 4.13: D+5 Market vs SVI Implied Vols. Comparison for DAX Call Options

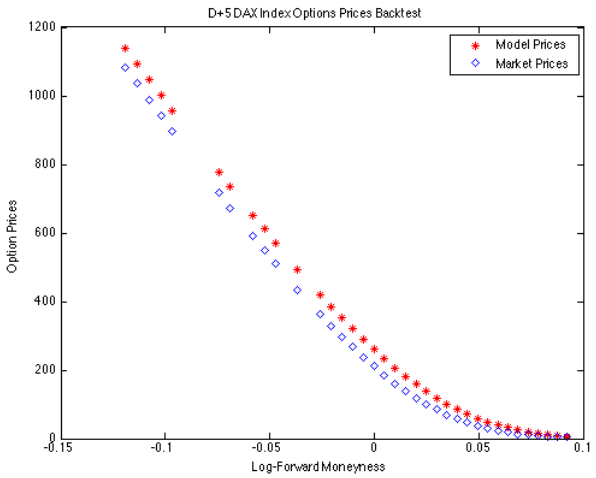

Figure 4.14: D+5 Market Prices vs Model Prices Comparison for DAX Call Options

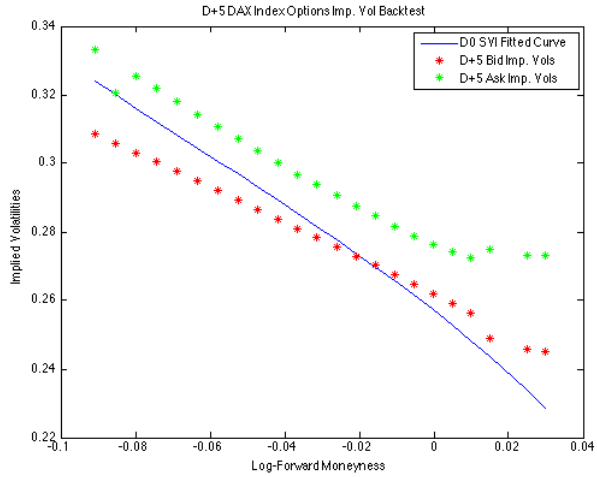

Figure 4.15: D+5 Market vs SVI Implied Vols. Comparison for DAX Put Options

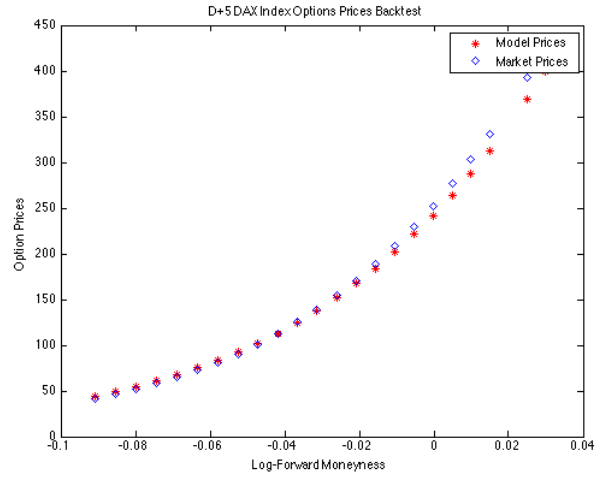

Figure 4.16: D+5 Market Prices vs Model Prices Comparison for DAX Put Options

4.3 SPX Index spot options

SPX Index Spot Options are negotiated at *Chicago Board Options Exchanged* and is the most liquid equity options in the world. The underlying currency is USD (American Dollar).

Figures 4.17 and 4.19 show fitted SVI curves for the SPX Index options expiring in 18-Mar-2016 and traded at 22-Jan-2016. As one can see through Figures 4.18 and 4.20, the SVI curves for call and put options are free of butterfly arbitrage.

	a	b	m	ρ	σ
SPX Index Spot Call Options	0.1998	0.1273	0.0644	-5.5263	0.0022
SPX Index Spot Put Options	0.2381	1.2779	0.0603	0.3069	0.0200

Table 4.3: Calibrated Parameters for SPX Index Options

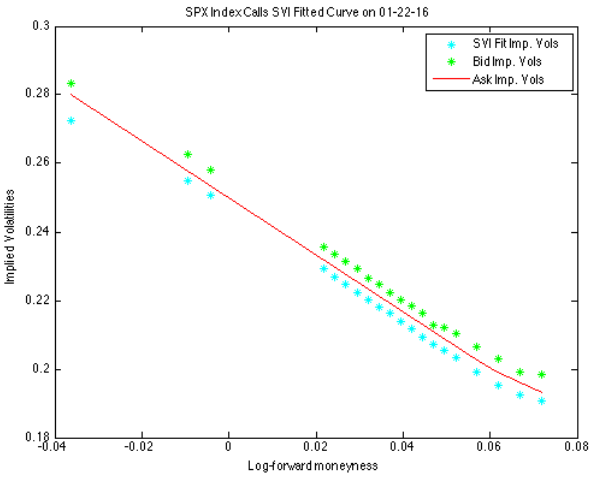

Figure 4.17: SPX Index Call Options' SVI Fitted Curve (expiring: March/16)

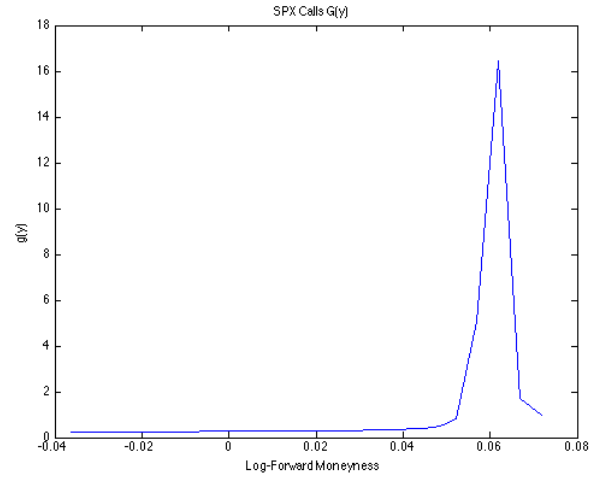

Figure 4.18: g(y) function for SPX Index Calls Options SVI Fit

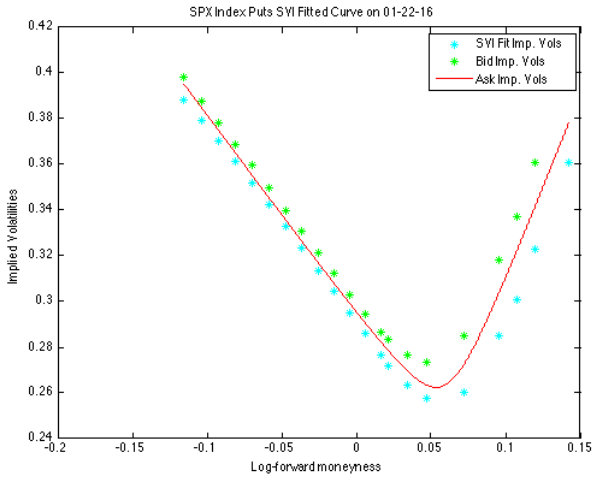

Figure 4.19: SPX Index Put Options' SVI Fitted Curve (expiring: March/16)

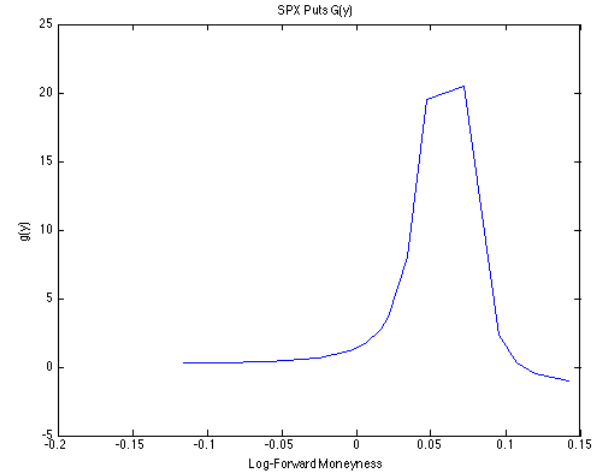

Figure 4.20: g(y) function for SPX Index Puts Options SVI Fit

4.3.1 Backtest Results for SPX Index Spot Options

Figures 4.22, 4.26, 4.30, 4.24, 4.28 and 4.32 show the comparison between market prices and the predicted prices at the dates $D+1$, $D+3$ and $D+5$. The predictions are evaluated with the SVI volatilities calibrated at D.

Figures 4.21, 4.25, 4.29, 4.23, 4.27 and 4.31 compares market implied volatilities of bid and ask prices and the volatilities of prices predicted by the SVI model.

As we can see in the figures and in Table 4.4 the prices given by the SVI model are close to the market ones, which means that, this model can be used to predict prices.

Calls	D+1	D+3	D+5
Data misfit for vols.	$1.23.10^{-1}$	$1.24.10^{-1}$	$1.53.10^{-2}$
Normalized ℓ_2-error of prices	$2.17.10^{-1}$	$2.11.10^{-1}$	$1.04.10^{-1}$
Average error over spot	$2.70.10^{-3}$	$2.50.10^{-3}$	$1.40.10^{-3}$
Puts	D+1	D+3	D+5
Data misfit for vols.	$7.93.10^{-2}$	$8.97.10^{-2}$	$6.05.10^{-2}$
Normalized ℓ_2-error of prices	$4.65.10^{-2}$	$9.42.10^{-2}$	$8.84.10^{-2}$
Average error over spot	$2.50.10^{-3}$	$4.40.10^{-3}$	$1.80.10^{-3}$

Table 4.4: Quantitative Indexes for SPX Index Options

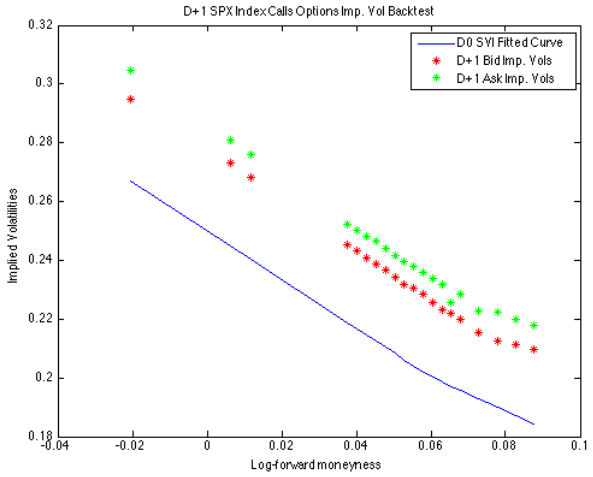

Figure 4.21: D+1 Market vs SVI Implied Vols. Comparison for SPX Call Options

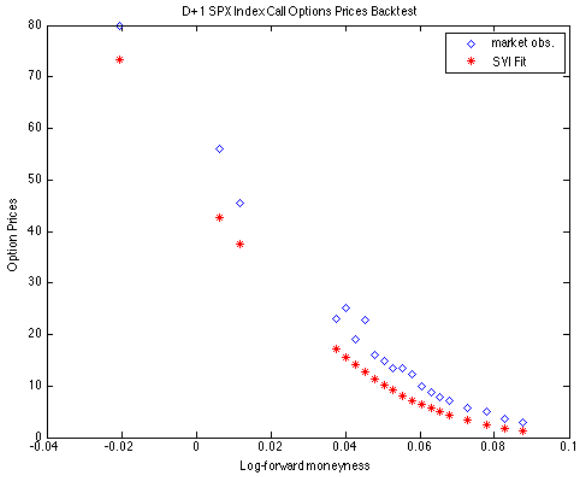

Figure 4.22: D+1 Market Prices vs Model Prices Comparison for SPX Call Options

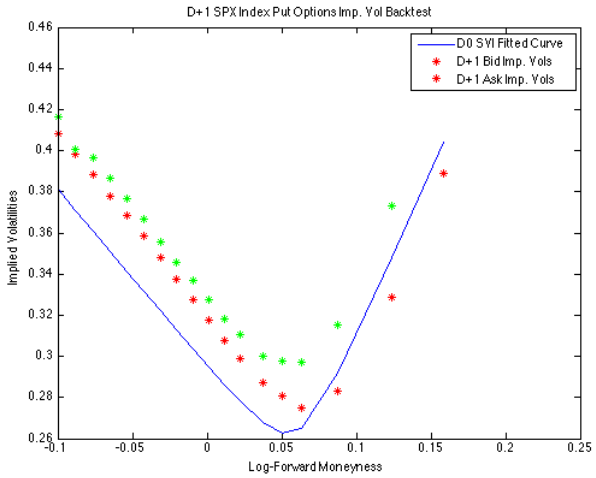

Figure 4.23: D+1 Market vs SVI Implied Vols. Comparison for SPX Put Options

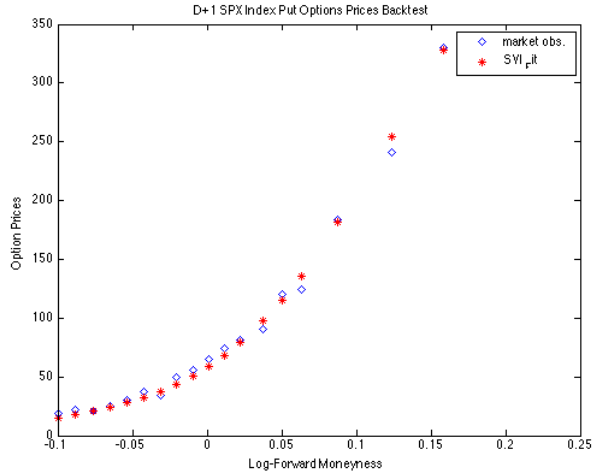

Figure 4.24: D+1 Market Prices vs Model Prices Comparison for SPX Put Options

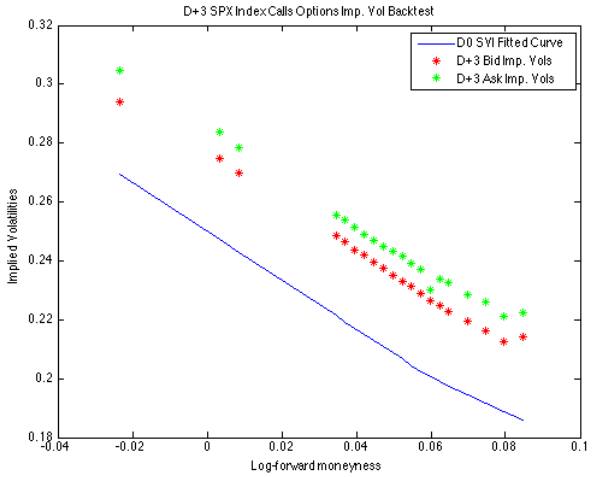

Figure 4.25: D+3 Market vs SVI Implied Vols. Comparison for SPX Call Options

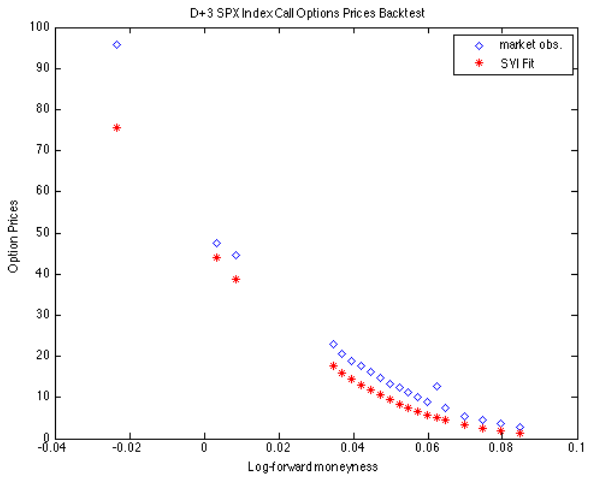

Figure 4.26: D+3 Market Prices vs Model Prices Comparison for SPX Call Options

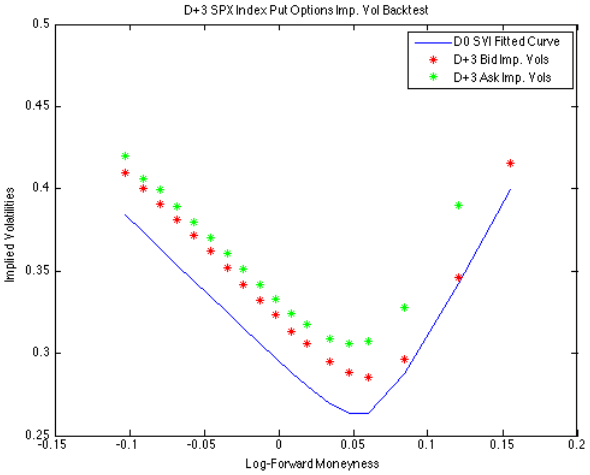

Figure 4.27: D+3 Market vs SVI Implied Vols. Comparison for SPX Put Options

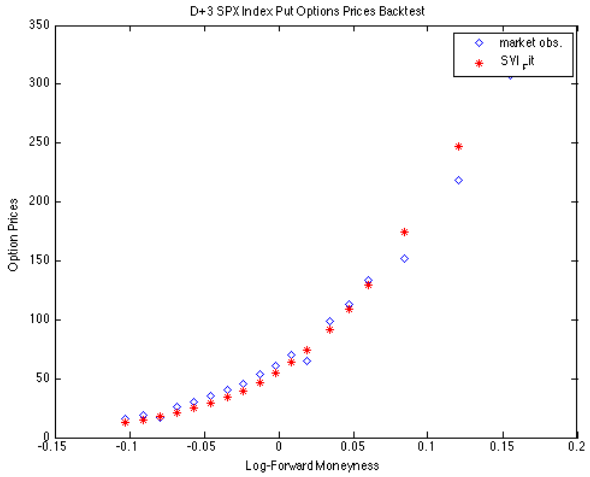

Figure 4.28: D+3 Market Prices vs Model Prices Comparison for SPX Put Options

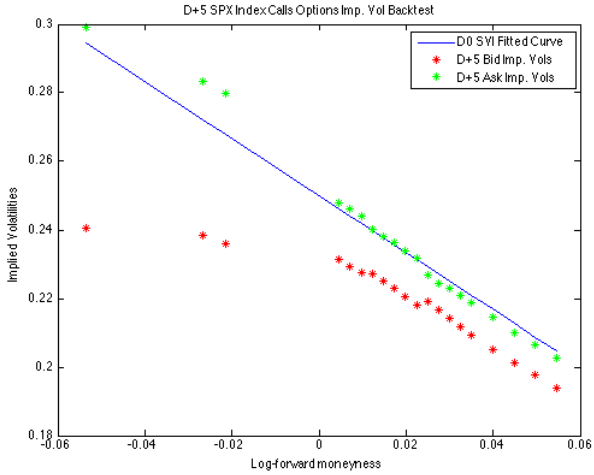

Figure 4.29: D+5 Market vs SVI Implied Vols. Comparison for SPX Call Options

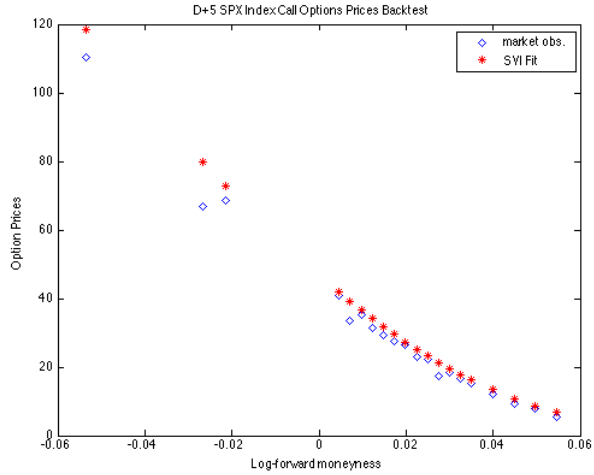

Figure 4.30: D+5 Market Prices vs Model Prices Comparison for SPX Call Options

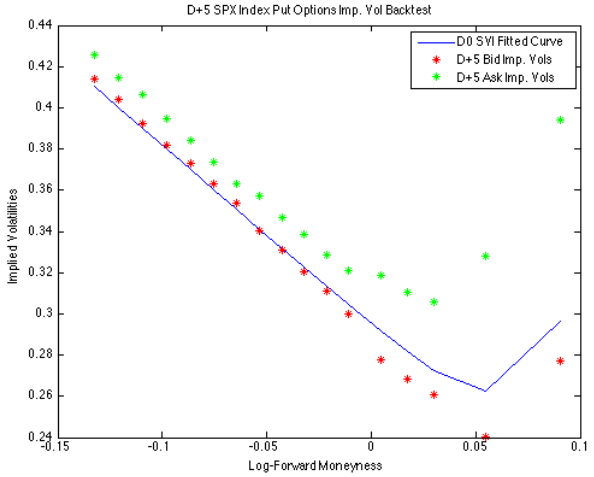

Figure 4.31: D+5 Market vs SVI Implied Vols. Comparison for SPX Put Options

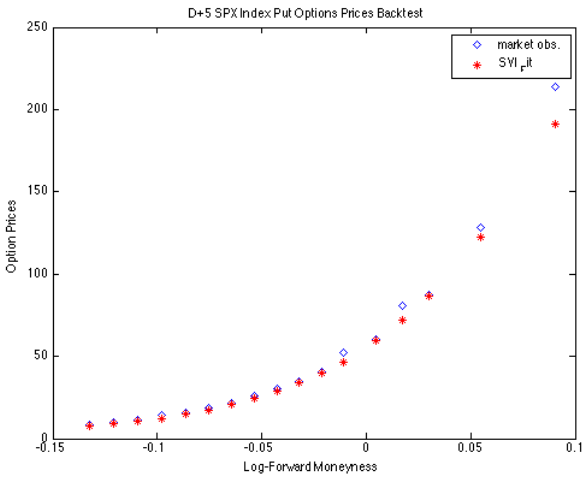

Figure 4.32: D+5 Market Prices vs Model Prices Comparison for SPX Put Options

4.4 PETR4 Equity Options

Petrobras PN equity options are the most liquid equity options in Brazil. They are negotiated at *BMF&Bovespa Stock Exchange* in BRL (Brazilian Reais). The volume of daily trading for these options are not as big as the ones in the examples above, which can give us less accurate results.

Figures 4.33 and 4.35 show fitted SVI curves for PETR4 Equity options expiring in 21-Mar-2016 and traded at 5-Feb-2016. As one can see in Figures 4.34 and 4.36, both SVI curves are free of butterfly arbitrage.

	a	b	m	ρ	σ
PETR4 Equity Call Options	0.1998	0.1273	0.0644	-5.5263	0.0022
PETR4 Equity Put Options	0.2381	1.2779	0.0603	0.3069	0.0200

Table 4.5: Calibrated Parameters for PETR4 Index Options

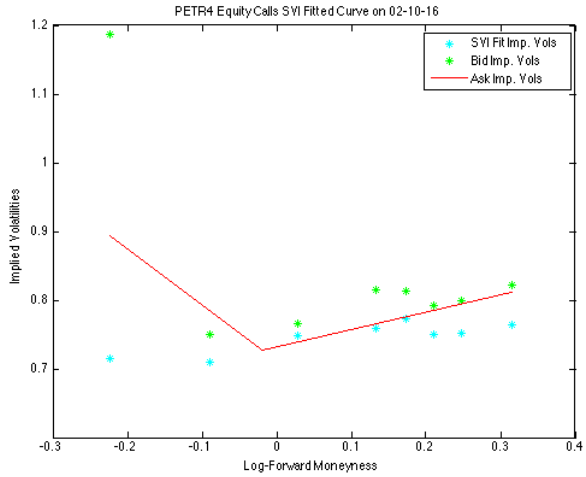

Figure 4.33: PETR4 Equity Call Options' SVI Fitted Curve (expiring: March/16)

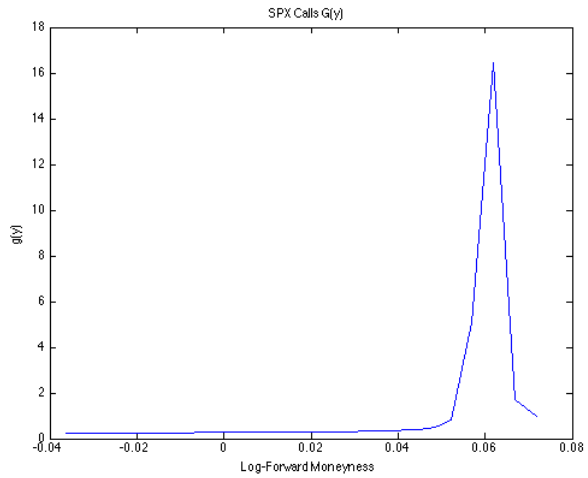

Figure 4.34: g(y) function for PETR4 Equity Calls Options SVI Fit

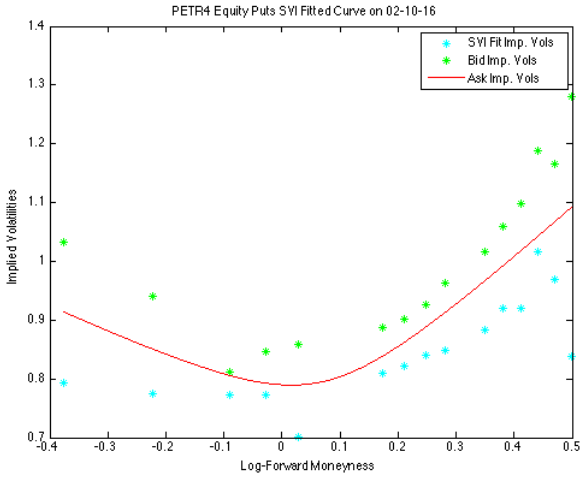

Figure 4.35: PETR4 Equity Put Options' SVI Fitted Curve (expiring: March/16)

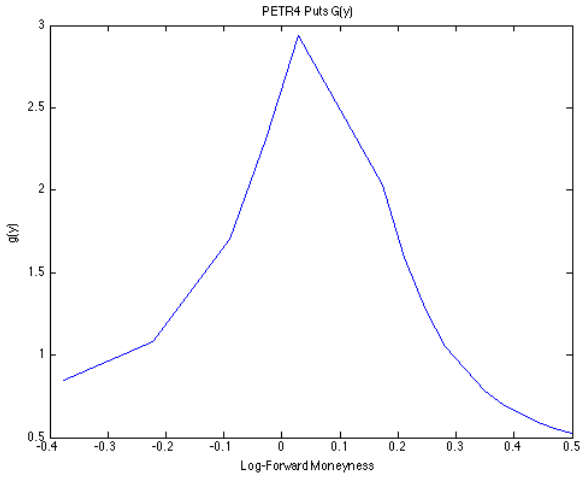

Figure 4.36: g(y) function for PETR4 Equity Puts Options SVI Fit

4.4.1 Backtest Results for PETR4 Equity Options

Figures 4.38, 4.42, 4.46, 4.40, 4.44 and 4.48 show the comparison between market prices and the predicted prices at the dates $D+1$, $D+3$ and $D+5$. The predictions are evaluated with the SVI volatilities calibrated at D.

Figures 4.37, 4.41, 4.45, 4.39, 4.43 and 4.47 compares market implied volatilities of bid and ask prices and the volatilities of prices predicted by the SVI model.

As we can see in Table 4.6, the predictions are less accurate than in the previous examples, probably due to the smaller amount of data and the smaller trading volume. However the predicted prices presented skewness similar to the market ones, which is a nice feature.

Calls	D+1	D+3	D+5
Data misfit for vols.	$1.23.10^{-1}$	$1.24.10^{-1}$	$1.53.10^{-2}$
Normalized ℓ_2-error of prices	$2.17.10^{-1}$	$2.11.10^{-1}$	$1.04.10^{-1}$
Average error over spot	$2.70.10^{-3}$	$2.50.10^{-3}$	$1.40.10^{-3}$
Puts	D+1	D+3	D+5
Data misfit for vols.	$7.93.10^{-2}$	$8.97.10^{-2}$	$6.05.10^{-2}$
Normalized ℓ_2-error of prices	$4.65.10^{-2}$	$9.42.10^{-2}$	$8.84.10^{-2}$
Average error over spot	$2.50.10^{-3}$	$4.40.10^{-3}$	$1.80.10^{-3}$

Table 4.6: Quantitative Indexes for PETR4 Index Spot Options

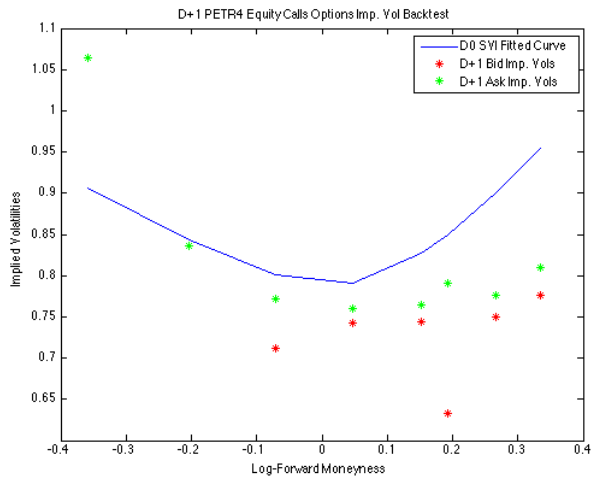

Figure 4.37: D+1 Market vs SVI Implied Vols. Comparison for PETR4 Call Options

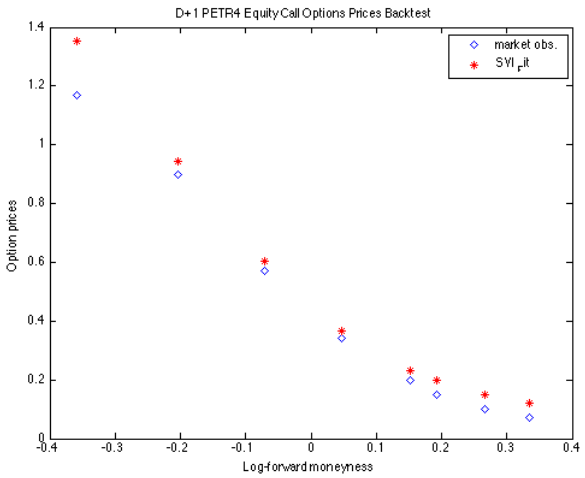

Figure 4.38: D+1 Market Prices vs Model Prices Comparison for PETR4 Call Options

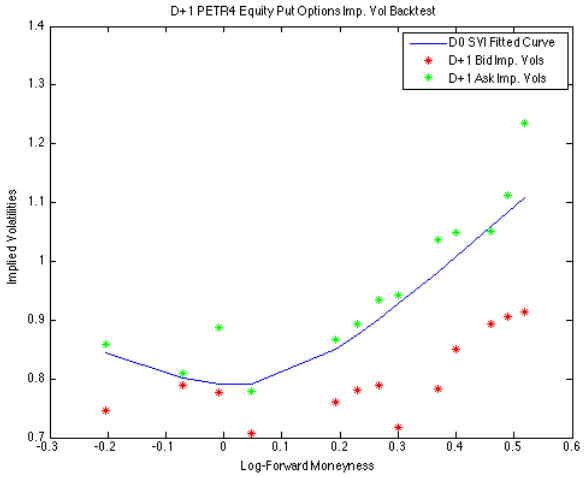

Figure 4.39: D+1 Market vs SVI Implied Vols. Comparison for PETR4 Put Options

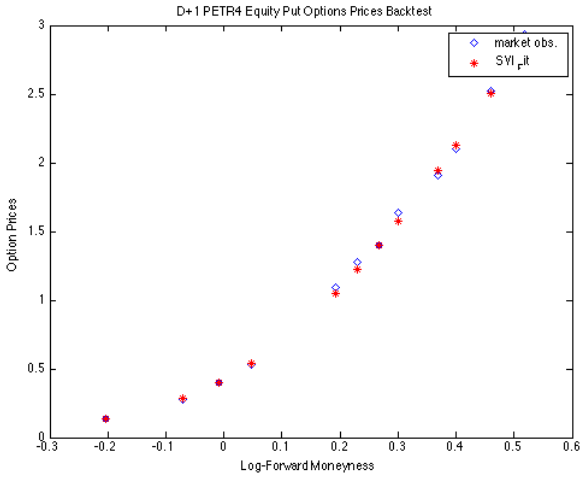

Figure 4.40: D+1 Market Prices vs Model Prices Comparison for PETR4 Put Options

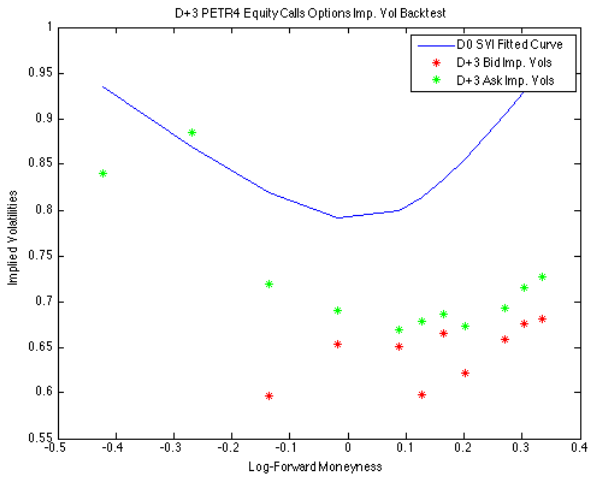

Figure 4.41: D+3 Market vs SVI Implied Vols. Comparison for PETR4 Call Options

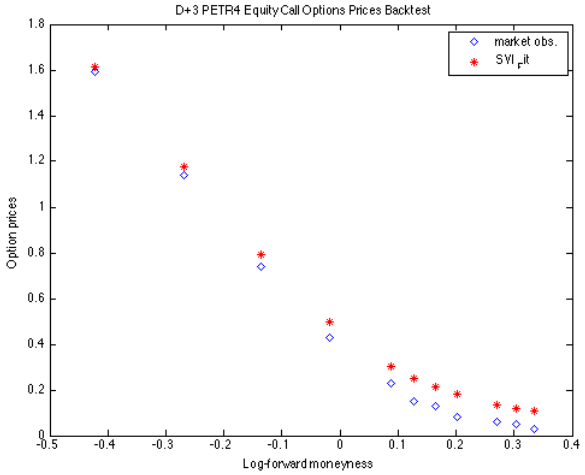

Figure 4.42: D+3 Market Prices vs Model Prices Comparison for PETR4 Call Options

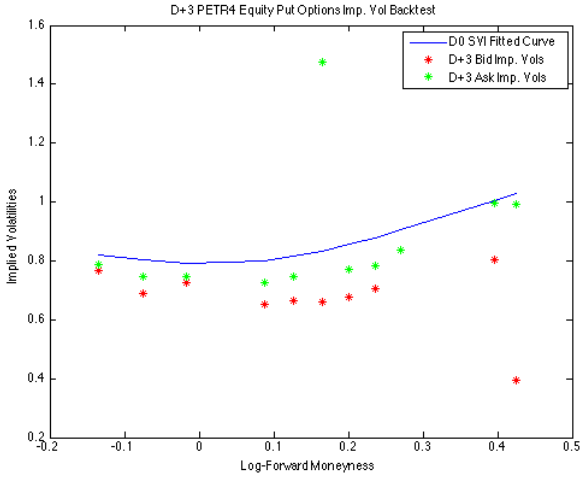

Figure 4.43: D+3 Market vs SVI Implied Vols. Comparison for PETR4 Put Options

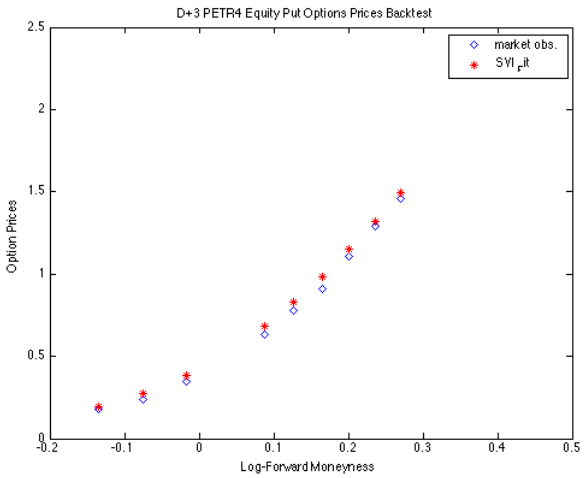

Figure 4.44: D+3 Market Prices vs Model Prices Comparison for PETR4 Put Options

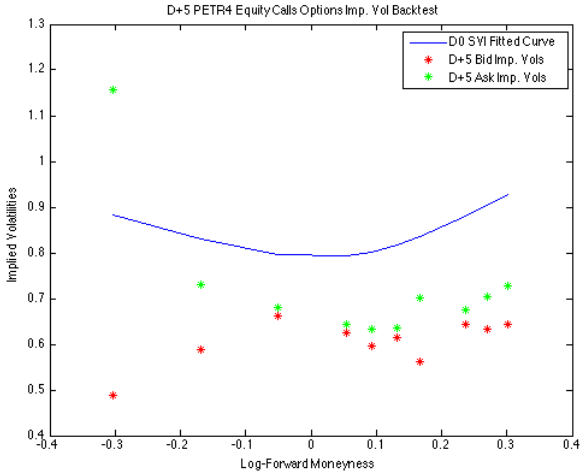

Figure 4.45: D+5 Market vs SVI Implied Vols. Comparison for PETR4 Call Options

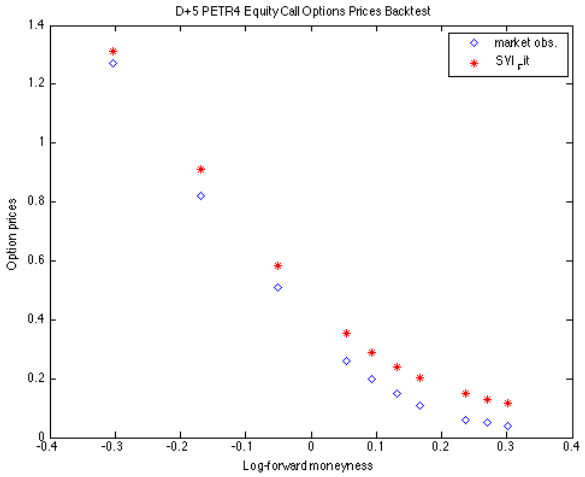

Figure 4.46: D+5 Market Prices vs Model Prices Comparison for PETR4 Call Options

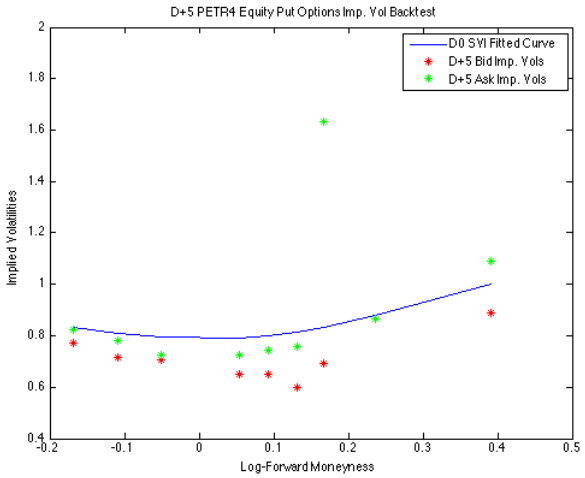

Figure 4.47: D+5 Market vs SVI Implied Vols. Comparison for PETR4 Put Options

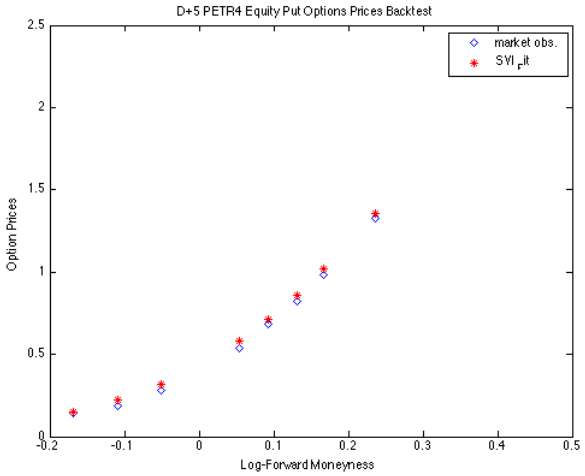

Figure 4.48: D+5 Market Prices vs Model Prices Comparison for PETR4 Put Options

4.5 Confidence Intervals

Although we are considering volatility as a deterministic function of the log-strike, we state confidence intervals, based on the bid-ask spread of option prices as follows:

- From D0 data, we evaluate the modulus of the difference between observed *bid-ask* implied volatilities, take the maximum over strikes and denote this quantity by δ.
- Denoting the SVI curve at each *log-strike* k by $\Sigma_{SVI}(k)$, we consider $\Sigma_{SVI}(k) \pm \delta/2$ upper and lower bounds.
- We calculate Black-Scholes prices using such bounds on the volatility to define confidence intervals for the option prices.

4.5.1 Numerical Example

Now, we evaluate such confidence interval using the D+1 backtest data for DAX Index Calls 4.2.1.

$$\delta = 0.0423$$

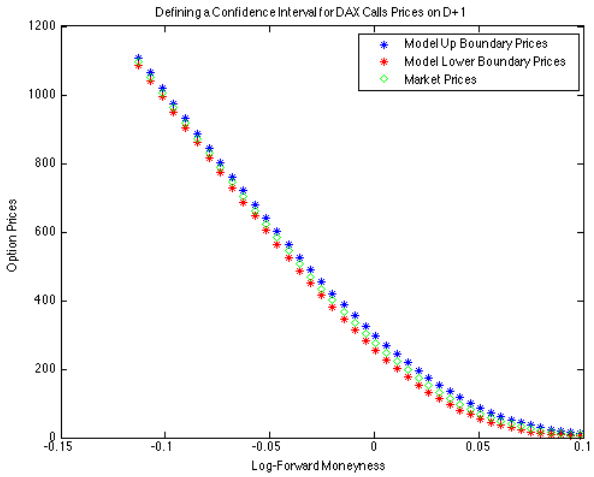

Figure 4.49: D+1 DAX Calls Prices Confidence Interval

We can also determine a confidence level for our interval by performing a Kupiec test [17] by determining the number of violations, i.e., the number of market prices outside the confidence interval. On the example above, the number of violations was 0 as we can see in Figure 4.50.

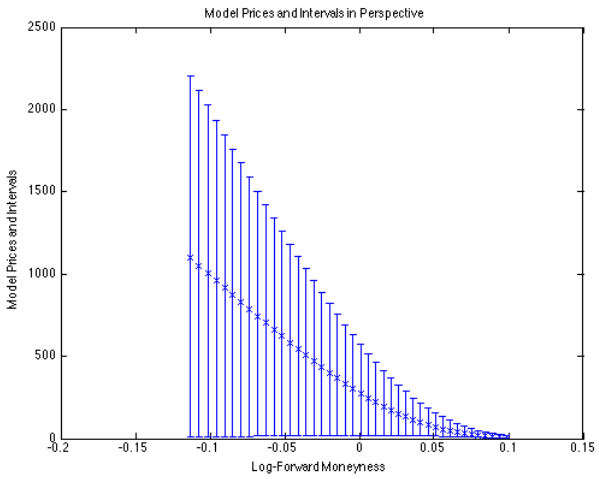

Figure 4.50: D+1 DAX Call Model Prices with its Confidence Intervals

4.6 An Alternative Approach

As an attempt to refine the technique proposed in Section 4.1, to forecast implied volatilities for the day $D + j$ with maturity time T, we evaluate, by an interpolation method, implied volatilities for the day D with maturity time $T - j$.

So, we use the two-dimensional interpolation method proposed in [15] and proceed as follows:

- Calculate implied volatilities smiles for several different expiring dates t_i (i a set of indexes for discrete time-to-maturity quantities) with data taken from the market;

- For each maturity $t \in [t_i, t_{i+1}]$ and strike K we calculate $\sigma^2_{imp}(K,t)t$ by interpolating linearly between $\sigma^2_{imp}(K,t_i)t_i$ and $\sigma^2_{imp}(K,t_{i+1})t_{i+1}$, where such values were obtained with SVI.

- So, we evaluate the surface of implied volatilities $(K,t) \mapsto \sigma^2_{imp}(K,t)$.

As an example, we calibrated the surface for SPX European Options with data taken from *@Bloomberg* in May,13th. The total variance and implied volatility surfaces can be seen in Figures 4.51 and 4.52:

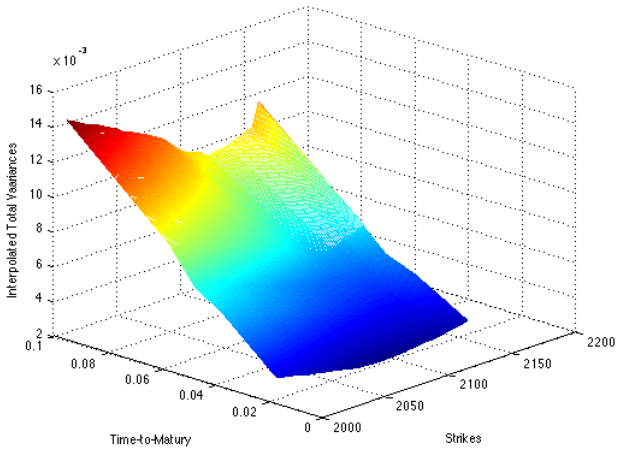

Figure 4.51: SPX European Calls - Interpolated Total Variance Surface

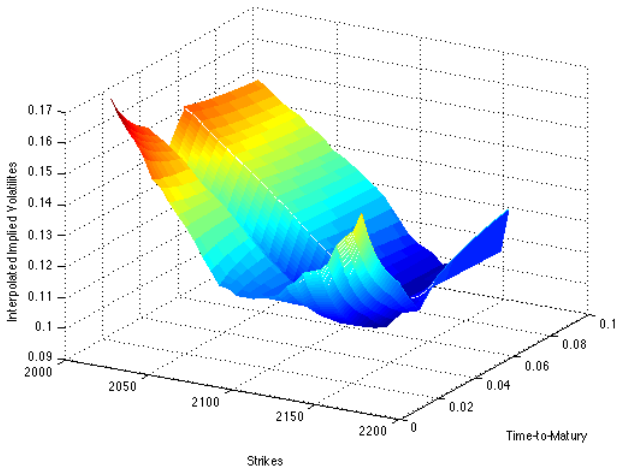

Figure 4.52: SPX European Calls - Interpolated Implied Volatilities Surface

As an example, we took market data on May, 18th for SPX calls expiring in May, 27th (j = 9). On the figure 4.53 you can find the SVI curve fitted with interpolated implied volatilities for D+j on May, 13th $\left(\sigma^2_{imp}(K,9)\right)$ as well as the bid and ask implied volatilities from market.

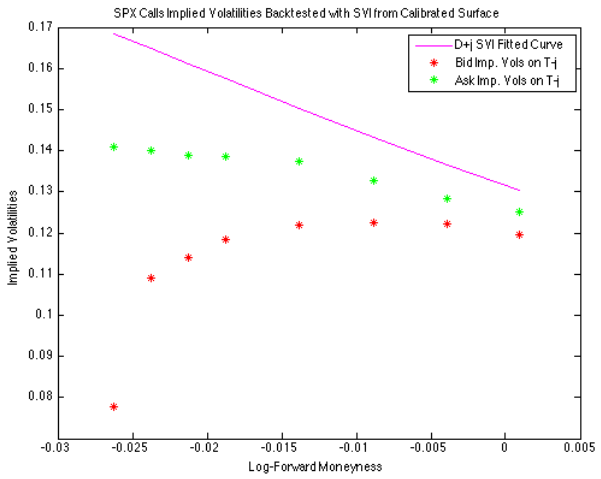

Figure 4.53: SVI Backtest with Interpolated Volatility Surface

Since the Data Misfit for the volatilities was $6.47x10^{-2}$, the single example above shows us no clear advantage in relation to the original experiment of the present work. However, we believe it's worth looking more carefully at it on posterior works.

Chapter 5

Concluding Remarks

In this work we intended to backtest SVI parameterization of Black-Scholes implied volatilities in order to see how accurate such model is to predict option prices.

After showing that SVI satisfies important non-arbitrage properties (see [18], [20], [11] and [13]), we presented an algorithm based on techniques from [22] to calibrate the SVI parameterized volatilities from market data. The algorithm included some modifications to increase the robustness of reconstructions, in order to be less dependent on the choice of the initial guess of the parameters m and σ. This provided us the necessary tools to start the backtest and perform the numerical examples presented in Chapter 4.

Finding reliable option data to test our algorithms was the first difficulty we faced. We had to gather all the necessary information about bid and ask prices of European options, choosing the ones with high trading volume. Thats why we have chosen DAX (EUREX), SPX (CBOE) and PETR4 (BMF&Bovespa) vanilla options.

A visual way to evaluate how accurate are the calibrated SVI curves is to observe its position in relation to market implied volatilities. Under this perspective, SVI parameters did not produced accurate predictions for all strikes, specially those far from the at-the-money, however, it predicted important features presented by the market data, such as skewness. So, this model can be advantageous for practitioners since it is computationally cheaper than stochastic volatility models.

Moreover, using SVI functional forms to price options for future scenarios might be an interesting tool in portfolio optimization techniques, such as the Black-Litterman inspired one, where the user inserts returns expectations into the model. See [1]. Going further on this research, we would like to suggest the same kind of test with smaller time frames in order to find out if it is possible to better understand how the volatilities react considering marginal disturbs on other variables.

Appendix

MATLAB Code for Quasi-Explicit SVI Calibration

```
function [a, b, rho, m, sigma, rmse] = SVI_fit(bid_vols,ask_vols,T,log_strikes)



%defining variables
mid_vols = (ask_vols + bid_vols)/2;
mid_total_vol = mid_vols*T;
n = length(mid_vols);
parameters_matrix = zeros(9801,6);
u=0;
for m_initial = 0.01 : 0.01 : 0.99
    for sigma_initial = 0.01 : 0.01 : 0.99


        % changing variable

        log_strikes_chg = (log_strikes - m_initial)/sigma_initial;
        mid_total_vol = mid_vols*T;

        % Solving the linear system to reach zero for the cost function.

        A = [n sum(log_strikes_chg) sum(sqrt(log_strikes_chg.^2+1));
            sum(log_strikes_chg) sum(log_strikes_chg.^2)
            log_strikes_chg'*sqrt(log_strikes_chg.^2 +1);
            sum(sqrt(log_strikes_chg.^2 +1)) log_strikes_chg'*sqrt(log_strikes_chg.^2 +1)
            sum(log_strikes_chg.^2 +1)];

        z = [sum(mid_total_vol); mid_total_vol'*log_strikes_chg;
            mid_total_vol'*sqrt((log_strikes_chg.^2 +1))];

        Parameters = A\z;
        a_tilde = Parameters(1);
        d = Parameters(2);
        c = Parameters(3);


        a = a_tilde/T;
        b = c/(sigma_initial*T);
        rho = d/(b*sigma_initial*T);

        % Now, considering a, b and rho we will minimize the problem choosing m and
        % sigma
```

```
        i = 0;
        m_loop = m_initial;
        sigma_loop = sigma_initial;

            while i <10

            x = sym('x',[1 2]);


            obj_function = @(x) sum((a + b*(rho*(log_strikes - x(1)) +
            sqrt((log_strikes - x(1)).^2 + x(2)^2)) - mid_vols).^2);

            x = fminsearch(obj_function,[m_loop , sigma_loop]);

            m_loop=x(1);
            sigma_loop=x(2);
            i=i+1;
            end
          m=m_loop;
          sigma=sigma_loop;

          fitted_values =   a + b*(rho*(log_strikes - m) +
          sqrt((log_strikes - m).^2 + sigma^2));

          lqs = sum((mid_vols - fitted_values).^2);

          u=u+1;
          parameters_matrix(u,1)=a;
          parameters_matrix(u,2)=b;
          parameters_matrix(u,3)=rho;
          parameters_matrix(u,4)=m;
          parameters_matrix(u,5)=sigma;
          parameters_matrix(u,6)=lqs;
    end
end

% defining m and sigma looking for the least square errors sum

min_error = min(parameters_matrix(:,6));
n = length(parameters_matrix);
for r = 1:n;
        if parameters_matrix(r,6) == min_error
            a = parameters_matrix(r,1);
            b = parameters_matrix(r,2);
            rho = parameters_matrix(r,3);
            m = parameters_matrix(r,4);
            sigma = parameters_matrix(r,5);
            rmse = sqrt(parameters_matrix(r,6));
        end
end
% graphic construction for visual analysis

liminf = min(log_strikes);
limsup = max(log_strikes);
x_axis= linspace(liminf,limsup,10000);
fitted_curve = a + b*(rho*(x_axis - m) + sqrt((x_axis - m).^2 + sigma^2));
plot(log_strikes,bid_vols,'c*');
```

```
hold on
plot(log_strikes,ask_vols,'g*');
plot(x_axis,fitted_curve,'r');
xlabel('Log-forward moneyness');
ylabel('Implied Volatilities');
legend('SVI Fit Imp. Vols','Bid Imp. Vols','Ask Imp. Vols');
hold off
```

MATLAB Code for Arbitrage Tests over Fitted Parameters

```
function [Result_BA, Result_RL] = SVI_Arbitrage_test( a, b, m, rho, sigma, log_strikes,T )

% This function tests the SVI calibrated curves for the non-arbitrage
% conditions

% Butterfly Arbitrage test:
n = length(log_strikes);
SVI = a + b*(rho*(log_strikes-m) + sqrt((log_strikes-m).^2 + sigma^2));
SVI_d1 = zeros(n,1);
SVI_d2 = zeros(n,1);
G_func = zeros(n,1);
for i = 1: n
     aux_1 = (log_strikes(i) - m );
     aux_2 = aux_1^2 + sigma^2;
     SVI_d1(i) = b*rho + b*aux_1/sqrt(aux_2);
     SVI_d2(i) = b*(sqrt(aux_2) - (aux_1^2)/sqrt(aux_2))/aux_2;

     G_func(i) =  (1 - log_strikes(i)*SVI_d1(i)/(2*SVI(i)))^2 -
     ((SVI_d1(i)^2) /4) *(1/SVI(i) + 1/4)+ SVI_d2(i)/2;
end

if min(G_func)<0 || min(SVI_d2)<0 ;

        Result_BA = 'The curve is not free of butterfly arbitrage';
else
        Result_BA = 'The curve is free of butterfly arbitrage.';
end

% Roger Lee Moments Condition test

BetaR = SVI(n)*T/abs(log_strikes(n));
BetaL = SVI(1)*T/abs(log_strikes(1));

if abs(BetaR)<2 && abs(BetaL)<2 ;
    Result_RL = 'The extreme slopes respect Roger Lee Moments Formula';
else
    Result_RL = 'The extreme slopes do not respect Roger Lee Moments Formula';
end

plot(log_strikes,G_func);
xlabel('Log-Forward Moneyness');
ylabel('g(y)');
```

Bibliography

[1] Fischer Black and Robert Litterman, *Asset Allocation combining Investor Views with Market Equilibrium*, The Journal of Fixed Income **1** (1991), no. 2, 7–18.

[2] Fischer Black and Myron Scholes, *The Pricing of Options and Corporate Liabilities*, Journal of Political Economy **81** (1973), no. 3, 637–654.

[3] P. Buchen and M.Kelly, *The Maximum Entropy Distribution of an Asset Inferred from Option Prices*, J. Financ. Quant. Anal. **31** (1996), 143–159.

[4] Stephane Crepey, *Calibration of the local volatility in a generalized Black-Scholes model using Tikhonov regularization*, SIAM Journal of Mathematical Analysis **34** (2003), 1183–1206.

[5] Emanuel Derman and Iraj Kani, *Riding on a Smile*, Risk **7** (1994), 32–39.

[6] Bruno Dupire, *Pricing With a Smile*, Risk Magazine **7** (1994), 18–20.

[7] Herbert Egger and Heinz Engl, *Tikhonov Regularization Applied to the Inverse Problem of Option Pricing: Convergence analysis and Rates*, Inverse Problems **21** (2005), 1027–1045.

[8] Heinz Engl, Martin Hanke, and Andreas Neubauer, *Regularization of Inverse Problems*, Mathematics and its Applications, vol. 375, Kluwer Academic Publishers Group, Dordrecht, 1996.

[9] Matthias Fengler, *Arbitrage-Free Smoothing of the Implied Volatility Surface*, Quantitative Finance **9** (2009), no. 4, 417–428.

[10] Jim Gatheral, *A Parsimonious Arbitrage-Free Implied Volatility Parameterization With Application to the Valuation of Volatility Derivatives*, To appear in Presentation of Global Derivatives, 2004.

[11] ———, *The Volatility Surface: A Practitioner's Guide*, Wiley Finance, 2006.

[12] Jim Gatheral and Jaquier A, *A Convergence of Heston to SVI*, Quantitative Finance **11** (2011), 1129–1132.

[13] Jim Gatheral and Antoine Jacquier, *Arbitrage-Free SVI Volatility Surfaces*, Quantitative Finance **14** (2014), no. 1, 59–71.

[14] Nabil Kahalé, *An Arbitrage-Free Interpolation of Volatilities*, Risk **17** (2004), 102–106.

[15] Nabil Kahalé, *Smile Interpolation and Calibration of the Local Volatility Model*, Risk Magazine **1** (2005), 637–654.

[16] Ralph Korn and Elke Korn, *Option Price and Portfolio Optimization: Modern Methods of Mathematical Finance*, Graduate Studies in Mathematics, vol. 31, AMS, 2001.

[17] Paul H. Kupiec, *Techniques for Verifying the Accuracy of Risk Measurement Models*, The Journal of Derivatives **3** (1995), no. 2, 73–84.

[18] Roger W. Lee, *The Moment Formula for Implied Volatility at Extreme Strikes*, Mathematical Finance **14** (2004), 469–480.

[19] Cassio Neri and Lorenz Schneider, *Maximum Entropy Distributions Inferred from Option Portfolios on an Asset*, Financ. Stoch. **16** (2012), no. 2, 293–318.

[20] Michael Paul Veran Roper, *Implied Volatility: General Properties and Assymptotics*, Ph.D. thesis, The University of New South Wales, October 2009.

[21] Otmar Scherzer, Markus Grasmair, Harald Grossauer, Markus Haltmeier, and Frank Lenzen, *Variational Methods in Imaging*, Applied Mathematical Sciences, vol. 167, Springer, New York, 2008.

[22] Zelaide Systems, *Quasi-Explicit Calibration of Gatheral's SVI model*, Zelaide White Paper (2009), 1–10.

[23] Paul Wilmott, *Paul Wilmott on Quantitative Finance*, 2nd ed., John Wiley & Sons, 2000.